Final
Project Technical Report
of ISTC 2325p

Mechanisms of Formation and Structure of Chromophores of Fluorescent Proteins from Anthozoa species

(From 1 March 2002 to 28 February 2005 for 36 months)

Sergey Anatolyevich Lukyanov
(Project Manager)
Shemyakin - Ovchinnikov Institute of Bioorganic Chemistry, RAS

March 2005

This work was supported financially by USA and performed under the contract to the International Science and Technology Center (ISTC), Moscow.

REPORT DOCUMENTATION PAGE

Form Approved OMB No. 0704-0188

1. REPORT DATE *(DD-MM-YYYY)*	2. REPORT TYPE	3. DATES COVERED *(From – To)*
18-04-2005	Final Report	01-Mar-02 - 02-May-05

4. TITLE AND SUBTITLE

Mechanisms of Formation and Structure of Chromophores of Fluorescent Proteins from Anthozoa Species

5a. CONTRACT NUMBER
ISTC Registration No: 2325

5b. GRANT NUMBER

5c. PROGRAM ELEMENT NUMBER

6. AUTHOR(S)

Dr. Serguei Anatolyevich Lukyanov

5d. PROJECT NUMBER

5d. TASK NUMBER

5e. WORK UNIT NUMBER

7. PERFORMING ORGANIZATION NAME(S) AND ADDRESS(ES)

Shemyakin-Ovchinnikov Institute of Bioorganic Chemistry, RAS
16/10 Miklukho-Maklaya
Moscow 117997 GSP
Russia

8. PERFORMING ORGANIZATION REPORT NUMBER

N/A

9. SPONSORING/MONITORING AGENCY NAME(S) AND ADDRESS(ES)

EOARD
PSC 802 BOX 14
FPO 09499-0014

10. SPONSOR/MONITOR'S ACRONYM(S)

11. SPONSOR/MONITOR'S REPORT NUMBER(S)
ISTC 01-7020

12. DISTRIBUTION/AVAILABILITY STATEMENT

Approved for public release; distribution is unlimited.

13. SUPPLEMENTARY NOTES

14. ABSTRACT

This report results from a contract tasking Shemyakin-Ovchinnikov Institute of Bioorganic Chemistry, RAS as follows: The whole array of fluorescent proteins from Anthozoa species were described over the past few years. These proteins represent the GFP-like family according to their homology to the green fluorescent protein. Recently, it was shown that FPs red-shifted absorbance/fluorescense (red shifted as compared to GFP) is associated with at least two different chromophore types (9,11). Therefore. we consider a number of FPs to deserve classification based on the implicated chromophore structure. In this project we propose to divide FPs into subfamilies according to denatured protein spectral properties which reflect the type of the chromophore involved. More recently, we have cloned a number of FPs with far-red emission maxima (12). We anticipate that these proteins include chromophores of a novel type. The proposed project is aimed to identify the proteins with a novel type of chromophore, to determine their chromophore chemical structure, and to elucidate the mechanisms that are responsible for the development of chromophores of different types.

15. SUBJECT TERMS
EOARD, Biological And Medical Sciences, Biochemistry

16. SECURITY CLASSIFICATION OF:			17. LIMITATION OF ABSTRACT	18, NUMBER OF PAGES	19a. NAME OF RESPONSIBLE PERSON
a. REPORT	b. ABSTRACT	c. THIS PAGE			VALERIE E. MARTINDALE, Lt Col, USAF
UNCLAS	UNCLAS	UNCLAS	UL	51	19b. TELEPHONE NUMBER *(Include area code)* +44 (0)20 7514 4437

ISTC 2325p

Mechanisms of Formation and Structure of Chromophores of Fluorescent Proteins from Anthozoa species

(From 1 March 2002 to 28 February 2005 for 36 months)

Sergey Anatolyevich Lukyanov (Project Manager)
Shemyakin - Ovchinnikov Institute of Bioorganic Chemistry, RAS

The objective of this project is to investigate chemical structures and mechanisms of formation of chromophores within proteins of Green Fluorescent Protein (GFP) family. The project consisted of two general stages. During the first stage our efforts were aimed at the classification of new GFP-like proteins (based on a chromophore chemical structure) and screening of GFP-like proteins for identification of new subfamilies. The scope of our work during the first stage was set within the experiments at the whole protein level. At this stage, conventional biochemical methods were applied in search of novel type subfamilies. The main goal of the second stage of the Project was to bring the study up to the level of the chromophore fine chemical structure. For the second stage we have planned isolating chromophore-bearing peptides and studying their structure by ESI-mass-spectrometry, tandem mass-spectrometry and NMR.

Keywords (about 10 words) : fluorescent protein, chromophore, Anthozoa, coral, chromoprotein, denaturation kinetics, DsRed-subfamily, mass-spectrometry, nuclear magnetic resonance

*117997, Moscow, Miklukho-Maklaya 16/10, Russia
Phone +7-(095) 429-80-20, Fax +7-(095) 330-70-56
E-mail: luk@ibch.ru

ISTC 2325p

The work has been performed by
the following institutes and collaborators.

1. Participated institutes:
   1.1 Leading institute:

Shemyakin - Ovchinnikov Institute of Bioorganic Chemistry, RAS
117997, Moscow, Miklukho-Maklaya 16/10, Russia
Phone +7-(095) 429-80-20, Fax +7-(095) 330-70-56
E-mail: luk@ibch.ru

FINAL REPORT ON THE PARTNER PROJECT 2325p
"THE MECHANISMS OF FORMATION AND STRUCTURE OF CHROMOPHORES OF FLUORESCENT PROTEINS FROM *ANTHOZOA* SPECIES"

LIST OF CONTENTS

FINAL REPORT ON THE PARTNER PROJECT 2325p

THE MECHANISMS OF FORMATION AND STRUCTURE OF CHROMOPHORES OF FLUORESCENT PROTEINS FROM *ANTHOZOA* SPECIES

Shemiakin - Ovchinnikov Institute of Bioorganic Chemistry, RAS

Brief description of the work plan: objective, expected results, technical approach.

On the whole, this Project can be divided into two general stages. During the first stage of the Project our efforts were aimed at the classification of new GFP-like proteins (based on a chromophore chemical structure) and screening of GFP-like proteins for identification of new subfamilies. The scope of our work during the first stage was set within the experiments at the whole protein level. At this stage, conventional biochemical methods were applied in search of novel type subfamilies. The main goal of the second stage of the Project was to bring the study up to the level of the chromophore fine chemical structure. For the second stage we have planned isolating chromophore-bearing peptides and studying their structure by ESI-mass-spectrometry, tandem mass-spectrometry and NMR.

TECHNICAL PROGRESS.

Stage A. Classification of GFP-like proteins based on the chromophore structure.

According to the Work Plan, we have studied three chromoproteins (CPs), namely, *Heteractis crispa* (hc CP), *Condylactis gigantea* (cg CP) and *Goniopora tenuidens* (gt CP). Following directed mutagenesis all these chromoproteins were shown to emit light in the far-red region (emission λmax 615-645nm) We have analysed the wild forms of these chromoproteins, which are nonfluorescent and absorb light in the visible region (λmax 570-580nm).

Task 1. Spectral properties of different CPs upon denaturation.

GFP-like proteins display variable spectral properties spanning the visible spectrum. Apparently, spectral diversity results from different types of chromophores involved in protein structure and the way by which a chromophore interacts with its protein environment. In denatured state amino acid side chains do not interact with chromophore moiety, so that in denatured state protein visible spectrum exactly reflects the type of implicated chromophore structure. In the framework of this task we studied absorption properties of far-red CPs after denaturation in order to evaluate the type of chromophore implicated in these proteins.

Each of three far-red CPs retained their native absorption characteristics upon prolonged incubation at room temperature in 8M urea, 6M guanidine HCL, 1% sodium dodecyl sulfate or in the interval pH between 3 and 12. Other conditions commonly used for protein denaturation also did not change the native absorption spectra of these CPs. For example, organic solvents, such as 50% methanol did not cause denaturation at room temperature. Treatment with non-specific protease, pronase, did not affect either native absorption properties or mobility of protein bands in SDS/PAGE. In general, all far-red proteins proved to be the most resistant to denaturating conditions in the GFP-like proteins family. Only after boiling for 10-15 min. they

lost their native absorption characteristics. The thermal stability rose in the following row hcCP< cgCP< gtCP.

After heat-induced denaturation all three proteins could not be distinguished from each other on the basis of visible absorption spectroscopy. All heat-denatured CPs showed absorption maxima at 380nm at pH 3.0 and 450nm at pH14.0. This pH-dependant spectral transition is very similar to GFP chromophore after heat denaturation. Thus, we consider this evidence that the far-red CPs posess related to GFP chemical structures, with chromophore core based on GFP-like imidazolone ring. After alkaline denaturation (0.1 N NaOH, pH 14) absorption maxima of all CPs immediately shifted to 450nm. Further titration to the neutral and then to acidic conditions additionally shifted maxima to λmax 380nm. Alkaline denaturation, like heat-induced denaturation showed, that chromophore core of far-red proteins share common features with GFP chromophore.

Denaturation under the mild acidic conditions (pH 3.0) resulted in the more complex spectral changes. Initially, at pH 3.0 all three proteins showed the same absorption maximum at 448nm. Subsequent neutralization of 448nm-form resulted in complete renaturation of CPs, as monitored by absorption spectroscopy. Further incubation at pH 3.0 showed, that 448nm-form undergoes slow convertion to the 380nm form (1.5-2.5 hours, for different CPs) (Fig.1). Neutralization of the samples after different time of incubation resulted only in partial renaturation of proteins. The extent of renaturation corresponded to the ratio of 448nm to 380nm forms(not shown).

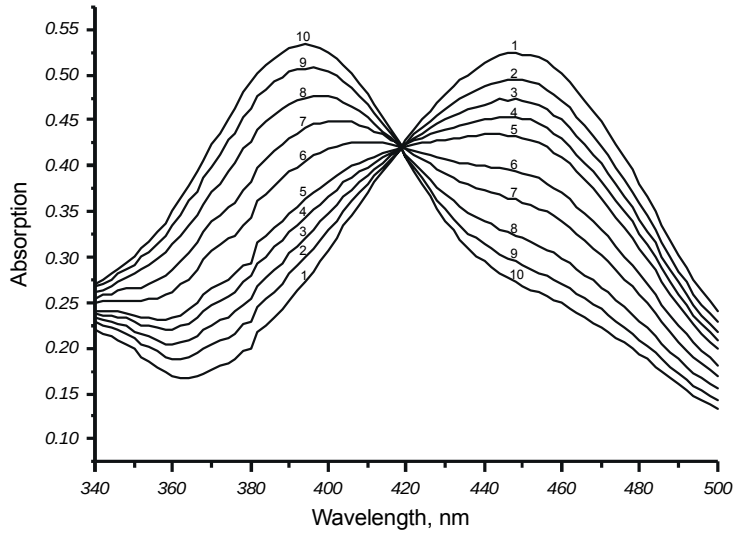

Figure 1. Spectral transformation of cgCP chromophore at pH 3.0. Spectra were taken after incubation of the protein at pH 3.0 for 1 min (1), 12 min (2), 22 min (3), 32 min (4), 42 min (5), 63 min (6), 83 min (7), 103 min (8), 122 min (9) and 142 min (10).

From these experiments we could draw the following conclusions:

First, all three far-red CPs include identical chromophores, which are based on GFP-like imidazolone structure. Under heat-induced denaturation, as well as after alkaline denaturation the chromophore of all proteins studied immediately converts to GFP-form, whereas at pH 3.0 this conversion is slower.

Second, in mild acidic conditions 448nm-form includes chemically intact chromophore structure, as judged by quantitative renaturation of this form.

Third, as far as 380nm-form did not revert to the native state in renaturation experiments, we consider that spectral transition from 448nm to 380nm-form coincides with a reaction of some labile bond essential for bathochromic shift of these proteins.

Similar situation was observed for the chromophore of DsRed, another GFP-like fluorescent protein. In DsRed a GFP-like imidazolone conjugated system is extended by additional acylimine bond. Hydration of this bond was shown to convert the red-shifted absorbing species back to GFP-like absorbance. Therefore, we decided to compare spectral behaviour of DsRed and far-red CPs upon acid-base induced denaturation. Under alkaline denaturation absorption maximum of DsRed immediately shifted to 452nm, similar to GFP and to far-red CPs. At pH 3.0 DsRed showed two maxima: at 380nm and 436nm (matured DsRed was reported to contain the green to red forms in approximately 1:1 ratio). The 436nm form further quickly (in 20 min) converted to 380nm form (Fig.2).

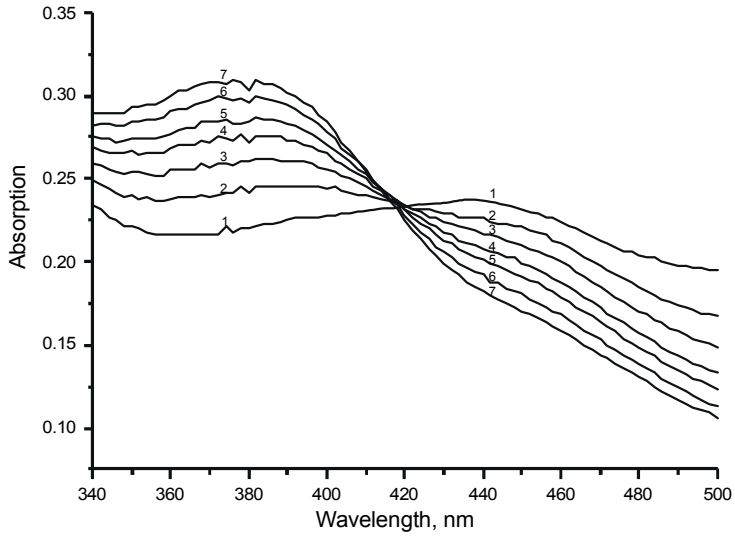

Figure 2. Spectral transformation of DsRed chromophore at pH 3.0. Spectra were taken after incubation of DsRed at pH 3.0 for 1 min (1), 3 min (2), 6 min (3), 9 min (4), 12 min (5), 17 min (6), 23 min (7).

Our interpretation of the results of spectral behaviour of DsRed and far-red CPs at pH 3.0 is that all the proteins contain a modified GFP-like imidazolone structure of the chromophore. This modification is most probably include a hydrolyzable bond which is in the native state of protein protected from the solvent within the polypeptide chain. Upon denaturation the protein shell is destroyed and this bond becomes hydrated followed by spectral transitions shown in Fig's 1 and 2. Hydration of a bond immediately abolishes the "red-shifting" modification of a chromophore and reverts its spectra to that ones very similar of GFP chromophore. Nevertheless, comparing spectral properties of DsRed and far-red CPs at pH 3.0 (Fig's 1 and 2) we observed different kinetics of spectral transitions and different absorption maxima of initially existing red forms. For this reason, we suggest that in far-red CPs chromophore moiety is modified by a bond different from acylimine as in DsRed.

Task 2. Spectrophotometric titration of denatured CPs.

The distinctive feature of chromophores of CPs from GFP-like proteins family is the presence of ionizable groups at the ends of conjugated system. Therefore, in denatured state CPs (FPs) display spectrally defined pH-

dependant forms, that are typical for a given chromophore structure. Upon titration these forms are interconvertable with pKa's characteristic for the chromophore type. It was shown earlier that GFP chromophore contains ionizable phenolic group with a pKa of 7.9-8.1 and a chromophore of asFP595 includes two such groups with pKa's of 6.8 and 10.9.

The far-red CPs proved to be extremely stable in the pH interval between 3 and 12. These properties, as well as these ones for other proteins from GFP-like family, derive from tightly packed three-dimensional structure that rigidly holds a chromophore within the protein core and protects the latter from exposure to surrounding solvents. To obtain the integral characteristics of a chromophore itself, such as pKa values, it is necessary to unfold the protein. Applying different conditions of unfolding one have to keep in mind that intact chromophores are likely to contain a hydrolysable bond. Therefore, not all the conditions of unfolding are applicable. In an ideal case, chromophore retains an intact chemical structure upon titration (448nm-form for far-red proteins at pH 3.0, see the previous report) and a protein does not undergo renaturation in the pH range of titration (pH 3-12).

To meet the first requirement all far-red CPs were denatured at pH 2.8, at the conditions generating transformation of proteins to 448nm-form. Titration of this form showed that above pH 3.5 all far-red CPs tend to renaturate and above pH 5.5 renaturation occurred instantly. To prevent renaturation, the samples were initially acidified to pH below 2.5, but at these conditions the 448nm-form with intact chromophore immediately converted to 380nm-form. Denaturation at pH 2.8 in the presence of 6M guanidine HCL or 8M urea or denaturation in the presence of the above reagents at elevated temperatures at neutral pH also resulted in complete transformation to 380nm-form. Therefore, we were unable to identify pKa's of intact "far-red" chromophore, due to rapid renaturation of 448nm-form at one conditions and loss of intactness of chromophore at the others.

As we have pointed out above, a 380nm-form of far-red CPs exists in one of two pH-dependent forms very similar to GFP chromophore (λmax 380nm at acidic pH and λmax 450nm at basic pH). But it could still be argued, that similar position of absorption maxima is merely a nonsignificant coincidence and a "far-red" chromophore has nothing in common with GFP-like imidazolone structure. To exclude this possibility a spectrophotometric titration of 380nm-form was done. Titration of far-red CPs denatured at pH 2.8 in the presence of 6M guanidine HCL showed a single isobestic point at 403nm and ionization of this form of chromophore with a pKa 7.9. These determined data nicely correlate with the values previously reported for the GFP chromophore. Thus, the above results support our finding, that a "far-red" chromophore share common features with GFP-like imidazolone structure.

Task 3. Electrophoretically determined fragmentation of CPs.

In the earlier papers GFP was shown to migrate as a single band in SDS/PAGE with Mr of 30.000. It was demonstrated later, that DsRed partially splits into fragments, the extent of fragmentation depending on the conditions of denaturation. Later, asFP595 was shown to exist predominantly in fragmented form, whatever conditions of denaturation were applied. All these data suggest that the conditions and the extent of fragmentation are characteristic features for a chromophore type of the GFP-like proteins.

In contrast with GFP, DsRed chromophore was reported to contain an extra double bond which is formed by an additional dehydrogenation at the second position of imidazolone. This acylimine bond is responsible for the red-shifted optical properties of DsRed. Upon

denaturation acylimine is hydrated and upon harsher treatment, especially at acidic conditions, acylimine bond hydrolyze. Hydrolysis of acylimine explains fragmentation of DsRed in SDS/PAGE. It should be mentioned, that mature DsRed contains "red" and "green" chromophores in approximately equal concentration. Therefore, fragmentation of DsRed does not exceed 50% of the total protein. asFP595, another protein from GFP-family, is amenable to fragmentation after autocatalytic cyclization of the chromophore along with the maturation of the protein. Therefore, the extent of fragmentation of asFP595 does not depend on the conditions of denaturation and exceeds 90%, as judged by SDS/PAGE

In attempts to identify chemical structure of "far-red' chromophore we proceeded from our finding, that it is composed of a modified imidazolone core. Thus, all the experiments were focused on a comparison of fragmentation of DsRed and far-red CPs upon different denaturating conditions. Noteworthy, the far-red CPs contain a chromophore in a predominantly"red" form, as it follows from the absence of 380nm-form initially after acid stimulated denaturation (see Fig.1). Therefore, assuming a "far-red" chromophore to contain the same as in DsRed acylimine bond, one would expect the fragmentation to considerably exceed 50% found for DsRed.

As it was expected, DsRed boiled in electrophoresis sample buffer showed two fragment bands in SDS/PAGE with apparent masses of 13 and 20 kDa and a major band of a full-length protein with Mr 30 kDa (Fig.3, laneA1). The extent of fragmentation of DsRed markedly increased when the protein was preboiled in 0.1M HCL (Fig.3, laneA2). The two "far-red" proteins, namely cgCP and hcCP, showed slightly increased fragmentation in 0.1M HCL(no more than 10% of the total protein, Fig.3, lanes B2 and C2), as compared to fragmentation of the same proteins boiled in electrophoresis sample buffer (Fig. 3, lanes B1 and C1). In contrast to cgCP and hcCP, *Goniopora tenuidens* CP showed a remarkable increase of the extent of fragmentation after preboiling in 0.1M HCL (80% of the overall protein, Fig.3, lane D2).

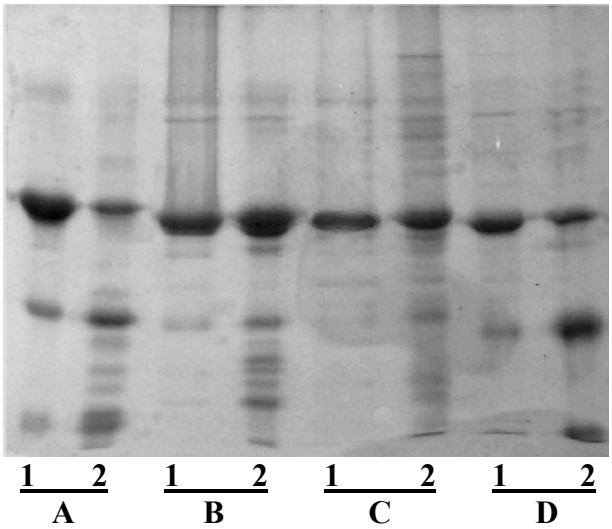

Fig. 3. Fragmentation of CPs detected by SDS/PAGE. Tracks 1. Proteins boiled in electrophoresis sample buffer for 5 min., Tracks 2. Proteins preboiled in 0.1M HCL for 5 min. and then boiled in the sample buffer. **A.** –DsRed, **B.** –cgCP, **C.** – hcCP, **D.** – gtCP.

Currently, our interpretation of the results of fragmentation of "far-red" proteins is that gtCP contain a chromophore of a DsRed-like structure, while chromophores of the two other "far-red" proteins cgCP and hcCP are of a different type. Nevertheless, two questions arise as far as

fragmentation results is concerned. First, assuming "far-red" CPs to contain a chromophore in predominantly "red" form it is clear, that the extent of fragmentation of gtCP might considerably exceed 50% found for DsRed. But still, there is no evidence that splitting of"far-red"proteins upon hydrolysis in 0.1M HCL occurs via "DsRed pathway", i.e. it is a hydrolysis of an acylimine bond that leads to fragmentation of "far-red" proteins. Second, if cgCP and hcCP comprise chromophores of different type as compared to DsRed and gtCP, and the bulk of the protein migrate in SDS/PAGE as a full length protein band, what is the reason for the rest of 10% of the protein to be cleaved. Besides, as we have found before, hydration and hydrolysis of a "red-shifting" bond is accompanied by complete conversion of 448nm-form to 380nm-form suggesting that the latter one would exist either in completely fragmented form (DsRed-like chromophore) or entirely as a full length protein (a chromophore without an acylimine).

One possible way to answer the first question is analysis of the products of hydrolysis of an acylimine substituted imidazolidinones. Carefully inspecting the structure of the product of complete hydrolysis of acylimine bond (as published by Tsien et al.) one can find an additional C=O electron withdrawing substituent . Therefore, it could be expected, that addition of water across C=N bond of acylimine would shift spectra back to GFP-like absorbance, but fully hydrolysed form of DsRed chromophore (with the cleaved 65-66 bond) might be red-shifted as compared to GFP denaturation products. Thus, a hydrolysis via "DsRed pathway" would lead to a spectrally defined form corresponding to 2-keto- derivative of imidazolidinone.

To check the last statement, the acylimine bond of DsRed was subjected to hydrolysis by boiling in 0.1M HCL, and the resulting suspension of denatured protein was clarified by trypsin digestion at pH 7.8. Finally, absorption spectra of the protein digest were taken. In comparison to the spectra of DsRed denatured at mild acidic conditions (finally exhibiting the two absorption peaks at pH7.8: 380nm and 450nm) the protein with completely hydrolysed acylimine bond clearly showed an additional shoulder at 530nm. Exactly as for DsRed similar experiments were carried out with "far-red" proteins. As shown for gtCP (Fig.4A) and cgCP (Fig.4B), the "far-red" CPs spectra also exhibited an absorption shoulder at 530nm.

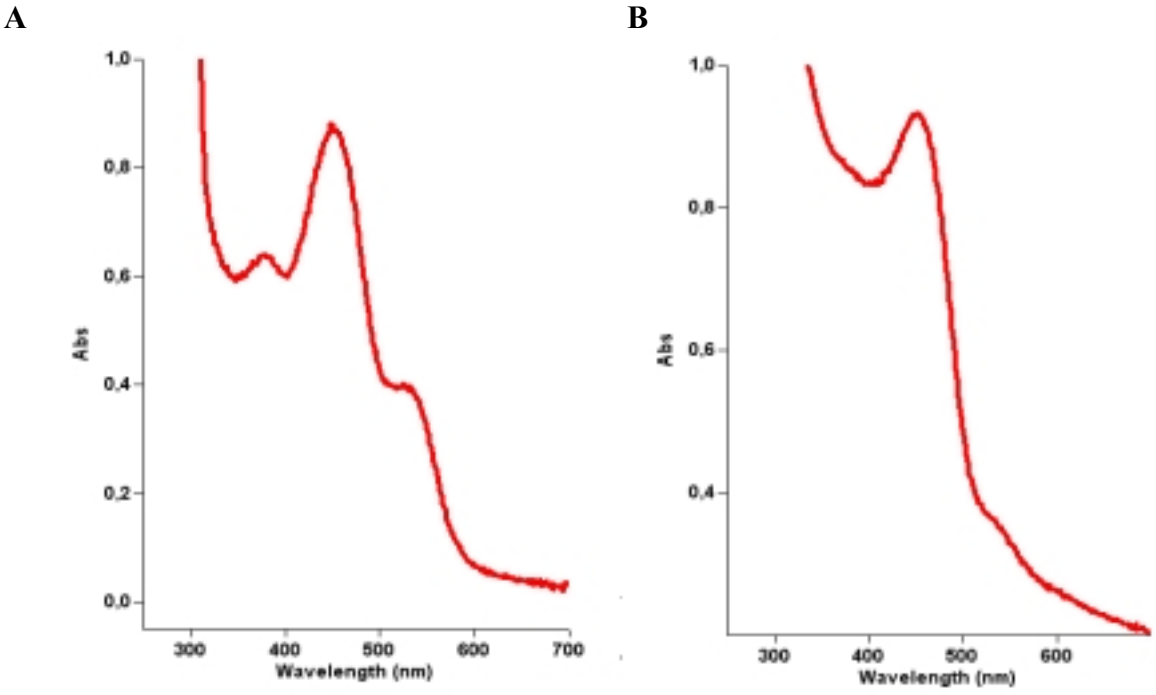

Fig. 4. Absorption spectra of gtCP (A) and cgCP (B) after complete hydrolysis of acylimine bond in 0.1M HCL.

Although the extinction of 2-keto- derivative was not determined, it is evident that the extent of fragmentation of gtCP and cgCP in SDS/PAGE correlate with the ratio of 530nm to 450nm absorbance in these spectra. The above results indicate that gtCP does include acylimine bond and no less than 4/5 of the total protein contains a chromophore in DsRed-like form. In contrast, cgCP contains only small portion of molecules with DsRed chromophore structure. Probably, an answer to the second above question is that maturation and synthesis of cgCP and hcCP chromophores proceeds via DsRed intermediate form (530nm absorbance corresponds to immature protein in this case), and gtCP include this form as a final product of synthesis.

Stage B. Screening of GFP-like proteins for identification of a novel type subfamilies.

Summing up the results discussed above the following attributives should be taken into account in classification of far-red proteins based on the type of chromophore structure:

- Upon different denaturating conditions far-red proteins finally show max. absorption at 380nm (pH 3.0) and 450nm (pH 14.0), indicating that far-red CPs share common features with GFP chromophore and include p-hydroxybenzylidene-imidazolone as a core structure of these proteins;

- Spectrophotometric titration of 380nm-form reveals the presence of ionizable group of far-red chromophore with a pKa 7.9. This value exactly corresponds to pKa of phenolic group of GFP chromophore;

- Upon denaturation at mild acidic conditions the “far-red” chromophore initially exists as 448nm-form which includes intact chromophore structure as judged by renaturation experiments. The 448nm-form further slowly converts to 380nm GFP-like form. We have explained this phenomenon as the lost of a “red-shifting” modification of far-red chromophore due to hydration of a bond which extends GFP-like chromophore conjugated system. The similar phenomenon was reported for DsRed chromophore earlier;

- An acylimine, a “red-shifting” modification of DsRed chromophore, is a very labile bond, which is prone to hydrolysis at harsh conditions. Therefore, fragmentation of the protein followed by hydrolysis of an acylimine at harsh conditions is a characteristic feature of DsRed chromophore. We have found that at these conditions *Goniopora tenuidens* CP predominantly exists in fragmented form (80%) but *Condylactis gigantea and Heteractis crispa* CPs show fragmentation to a much lesser extent (10%);

- The final product of an acylimine hydrolysis is a 2-keto-derivative of imidazolidinone. We have shown that formation of this derivative could be detected spectrophotometrically. The far-red CPs showed an absorption shoulder at 530nm, indicating that fragmentation of these proteins occurs via hydrolysis of an acylimine.

Considering the above criteria we have attributed gtCP to a DsRed subfamily according to the chromophore structure type. Although cgCP and hcCP share some common features with gtCP chromophore we suppose that these two ones belong to a new subfamily of GFP-like proteins with PCCXYGS motive in the chromophore-forming region.

Stage C. Determination of chromophore structure.

According to classification of far-red proteins proposed above, gtCP belongs to a subfamily of known chromophore structure. Both cgCP and hcCP, as we have shown, include identical chromophores of presumably new type. Therefore, at this stage we selected cgCP as an object to concentrate our efforts in further study of detailed chromophore structure.

Task 4. Optimization of the conditions for denaturation.

Condylactis gigantea chromoprotein, as well as other far-red CPs, proved to be extremely resistant to denaturating conditions. In 8M urea, 6M guanidine HCL, 1% SDS, some organic solvents or in the pH interval between 3 and 12 cgCP retained its native conformation. The most powerful nonspecific proteinases, such as pronase or proteinaseK failed to digest cgCP in its native state. On the other hand, cgCP chromophore was shown above to contain a labile bond providing for a red shift of this protein. Therefore, the aim of this part of work was a selection of compromise conditions for denaturation under which chromophore retains intactness.

It was shown before, that after heat-induced and alkaline denaturation cgCP irreversibly converts to 380nm- or 450nm-form. Other harsh denaturating conditions tested, also result in irreversible lost of a red-shifted absorption of cgCP chromophore. As we have shown before, cgCP chromophore temporarily conserves a red-shifting modification only at mild acidic denaturating conditions. In the pH range 3.0-3.3 the transformation of 448nm-form into 380nm-form at room temperature occurs for hours. At the same conditions denaturation kinetics is substantially slowed down and only a small portion of the protein exists in denatured state. Below pH 2.3 the protein denaturates instantly, but the life-time of 448nm-form is remarkably shortened. Therefore, we analyzed the behaviour of cgCP below pH 3.0 in order to find an optimal pH conditions for denaturation.

In the experiments on cgCP denaturation we detected the extent of denaturation by the absorption at 570nm since the protein in its native state absorbs maximally at this wavelength. The intactness of chromophore we followed by absorption at 448nm and the formation of GFP-like form of the chromophore was detected at 380nm. We have found that denaturation at pH 2.8 is optimal conditions for cgCP since absorption of the protein at 570nm drops instantly and conversion of 448nm-absorbance to 380nm-one occurs for several hours at room temperature.

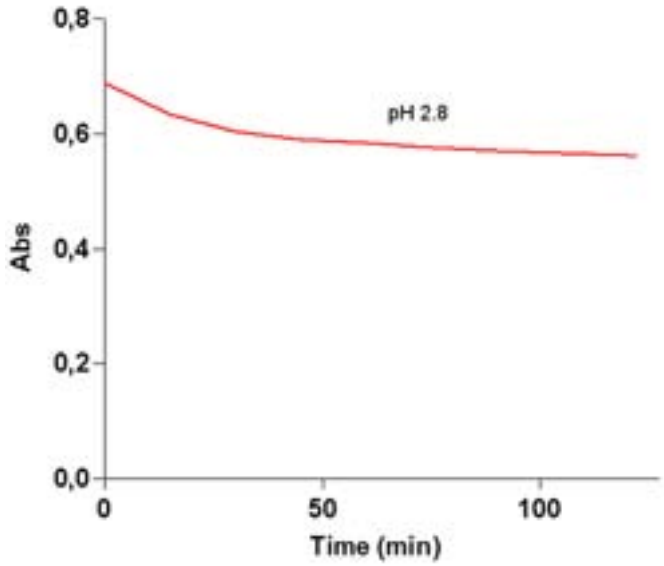

Fig. 5. Denaturation of cgCP at pH 2.8. The absorption of cgCP at 448nm was measured as a function of time.

Stage C. Determination of the chromophore structure.

Task 5. Digestion of denatured FPs by proteolytic enzymes.

Since denaturation at pH 2.8 had been found to be the optimal conditions for cgCP (report 4, task 4), a range of choice of enzymes suitable for proteolytic digestion was restricted to those ones showing optimum activity at acidic pHs. Therefore, we have chosen pepsin for proteolytic digestion of the denatured cgCP. Also, a limited life-time of a red-shifted form of denatured cgCP was taken into account, which temporarily maintained intact chromophore structure under denaturation conditions indicated above. Overnight digestion of denatured cgCP at pH 2.8 with pepsin led to disappearance of 448nm-form and complete conversion to a GFP-like 380nm-form. Thus, acid-induced denaturation followed by a short digestion (1h) with pepsin at high enzyme to protein ratio (1/10 w/w) at room temperature was selected as the method for generation of the chromophore-bearing proteolytic fragments, which retain a red-shifted absorbance. Obviously, one would have anticipated a limited proteolysis to occur at these conditions yielding a set of proteolytic chromophore-bearing fragments of different size. Nevertheless, as we expected some of these chromopeptides might retain an absorbance at 448 nm. To check this possibility cgCP was subjected to proteolysis at the conditions indicated above and after one hour proteolysis a digest was directly injected into HPLC chromatograph inlet and a peptide mixture was fractionated on a reverse-phase Ultrosphere ODS column. Peptides were eluted with a linear gradient of acetonitrile. The effluent was monitored both at 380 nm and 448 nm.

As shown in Fig. 6, limited proteolysis of cgCP with pepsin leads to a number of chromophore-bearing fragments of different size, which absorb solely at 380 nm. And although the total limited digest of cgCP retained an absorbance at 448 nm, no one chromophore-bearing fragment absorbing at 448 nm was detected upon HPLC fractionation. Our interpretation of the results of limited proteolysis of cgCP is that pepsin accelerates a 448 nm/380 nm conversion upon digestion. Alternatively, only 380 nm-form of cgCP is subjected to proteolysis. Anyway, we were unable isolating a cgCP chromophore-bearing fragment that retains a red-shifting modification. Therefore, at this stage of experiments we decided to study the structure of 380 nm-form of cgCP chromopeptide anticipating that these data would clarify the nature of a red-shifting modification of cgCP chromophore.

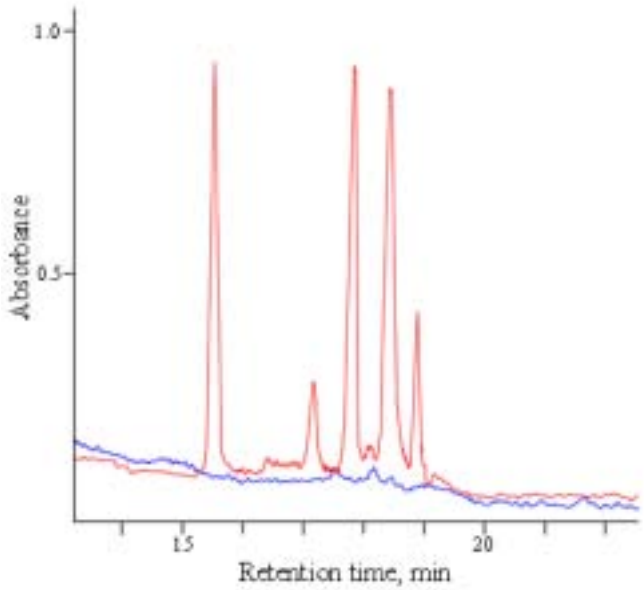

Fig. 6. HPLC fractionation of cgCP chromopeptides after limited proteolysis with pepsin. Absorbance of the effluent was monitored at 380 nm (red line) and 448 nm (blue line).

A green-to-red photoconvertable fluorescent protein from *Dendronephthya sp.*

A fluorescent protein from *Dendronephthya sp.* was recently cloned in our laboratory. This protein from GFP family manifests unique features after exposure to light. Originally it emits green light, but after illumination the red one. The color of the protein also changes from yellow to the red. Before illumination Dend FP absorbs maximally at 493nm with a shoulder at 470nm (Fig. 7). Irradiation of Dend FP with UV light shifts maximum of the absorbance to 557nm with a smaller peak at 520nm.

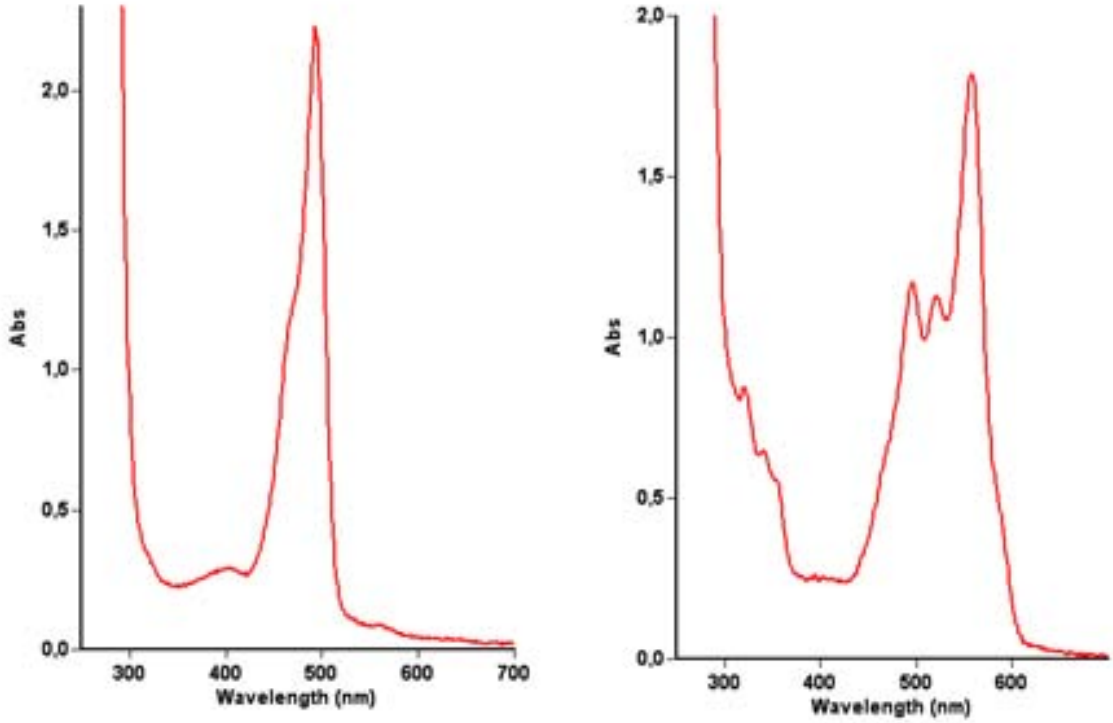

Fig. 7. Absorption spectra of Dend FP before illumination (left) and after exposure (right) to UV light (366nm) for 30 min.

Preliminary experiments with Dend FP spectral behaviour upon denaturation showed that unilluminated protein contains a chromophore very similar to GFP, as judged by spectral characteristics. Exposed to the light denatured Dend FP, as native protein itself, shows absorption maxima shift to longer wavelengths indicating that light induce a red-shifting modification in the chromophore structure of the protein. Because unlike other proteins from GFP family this one requires light to mature to the red state, we suppose that a mechanism of formation and structure of a chromophore of this protein must be quite different.

Tasks 1,2 UV-induced spectral changes of Dend FP

Purified on Ni-NTA agarose recombinant Dend FP showed a characteristic for many green-emitting proteins absorption spectrum with a maximum at 494 nm and a shoulder at 470 nm. After acid (0.1 M HCL) or alkaline (0.1 M NaOH) denaturation the protein showed maxima at 380 nm and 450 nm accordingly. These two forms (380 nm and 450 nm) of denatured Dend FP interconverted each into another in a pH-dependent manner, characteristic for the GFP chromophore. After exposition to the UV light, absorption at 494 nm of the native protein dropped and a new absorption maximum at 557 nm with a shoulder at 521 nm appeared. Unlike

denatured green protein, the denatured red Dend FP exhibited new pH-dependent forms with maxima at 430 nm and 500 nm. Illumination with UV-light also led to considerable changes in fluorescence spectra of the protein. Initially, Dend FP showed an emission maximum at 508 nm (Fig. 8A) which corresponds to the emission of the green light. After photoinduced conversion Dend FP emitted the bright-red light with an emission maximum shifted to 575 nm (Fig. 8B).

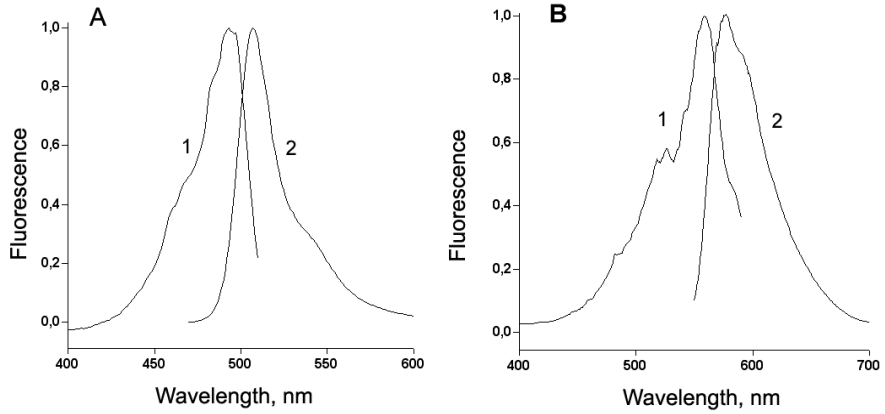

Fig. 8. Changes in fluorescence spectra upon photoconversion of Dend FP. Normalized excitation (1) and emission (2) spectra of the green (**A**) and red (**B**) forms of Dend FP.

Task 3 Electrophoretically determined fragmentation.

Originally, the green form of Dend FP migrated in SDS/PAAG as a single band of 28 kDa, characteristic for the full-length GFP-like proteins (Fig. 9, track 1). Upon exposition of the protein to the UV-light the intensity of 28 kDa band decreased and the two new fragments with masses of 18 kDa and 10 kDa formed (Fig. 9, track 2). Considering the masses of these two fragments and the position of chromophore-forming invariant aminoacids (X-Tyr-Gly) in the protein polypeptide chain, we assumed that photoinduced fragmentation of Dend FP occurs by splitting polypeptide chain nearby the chromophore center.

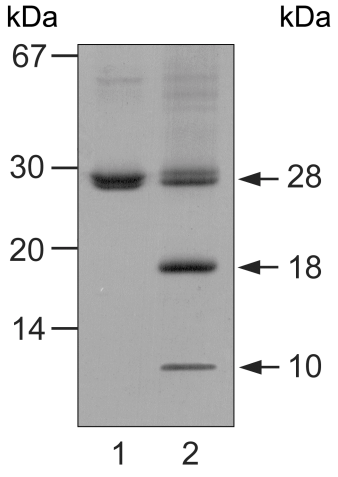

Fig. 9. Light-dependent fragmentation of Dend FP. Track 1 – the green form of Dend FP; Track 2 – the red form of the protein.

In DsRed subfamily of GFP-like proteins the red-shifted spectra derive from the additional dehydrogenation nearby the chromophore. The additional labile C=N double bond explains fragmentation of these proteins upon harsh denaturing conditions. Since Dend FP showed the

similar patterns of fragmentation, as judged by the same masses of fragments, the site of photoinduced cleavage of Dend FP must be located nearby the chromophore center.

Determination of oligomerization state of Dend FP

All GFP-like proteins display highly conserved, tightly packed tertiary structure and perhaps, this is the reason, why DsRed (the mass of tetrameric DsRed is 112 kDa) was eluted in the same volumes as bovine serum albumin (the mass 67 kDa) in gel-filtration experiments. Therefore, GFP-like proteins homologous to Dend FP were used in calibration of gel-filtration column (tetrameric DsRed and avGFP which was shown previously to be a monomer). Molecular mass of native Dend FP was determined separately for the green and red forms of the protein. Obtained in these experiments mass values suggested, that the native protein exhibits a dimeric structure and oligomerization state of the protein does not change upon photoconversion to the red form.

Tasks 4, 5. Optimization of the conditions of denaturation. Digestion of the denatured Dend FP by proteolytic enzymes.

Along with the spectral changes of the native protein, upon photoconversion to the red form, absorption spectra of the denatured red form of Dend FP also showed a considerable red shift, as compared to the spectra of the denatured green form. Unlike the green form, which exhibited the similar to GFP pH-dependent spectral forms with maxima at 380 nm and 450 nm, the red form of Dend FP showed new pH-dependent forms with absorption maxima at 430 nm (0.1 M HCl) and 500 nm (0.1 M NaOH). Since these two forms were found to be stable both at acidic and basic conditions, the protein was subjected to alkaline (0.1 M NaOH) denaturation before digestion with proteolytic enzymes. The denatured Dend FP was further subjected to trypsin digestion at pH 7.8.

Task 6. Isolation of the chromophore-bearing peptide of Dend FP.

Tryptic digest of Dend FP was directly applied onto HPLC reverse-phase Ultrosphere ODS column (4.5x250 mm), equilibrated with 10 mM sodium phosphate buffer pH 4.0. Peptides were eluted with a linear gradient of acetonitrile in 10 mM phosphate buffer pH 4.0. Peptide fractions were monitored both at 210 nm and 430 nm. The fraction absorbing at 430 nm was collected and further investigated in titration experiments. Spectrophotometric titration of the isolated Dend FP chromopeptide revealed the similar pH-dependent forms of the peptide (430 nm and 500 nm), as compared with the denatured red form of the protein. Thus, titration experiments evidenced, that the chromopeptide of Dend FP contains a chromophore structure in its intact form.

Task 8,9. Mass-spectral analysis of the isolated Dend FP chromopeptide.

All the attempts to elucidate the N-terminal aminoacid sequence of Dend FP chromopeptide by automatic aminoacid sequencing did not result in any sequence data. The negative sequence results suggested that polypeptide chain splits upon light-dependent green-to-red transformation of the protein and the loss of His65 α-NH_2 group is the result of the splitting. Therefore, in this situation we expected that mass-spectrometry experiments would help in aminoacid sequence determination. The Dend FP chromopeptide-containing fraction after HPLC was further analysed by ESI mass-spectrometry. ESI mass-spectra (Fig. 10) of Dend FP chromopeptide showed a

singular-charged molecular ion MH^+=609.3, which corresponded to the chromopeptide molecular mass of 608.3 Da.

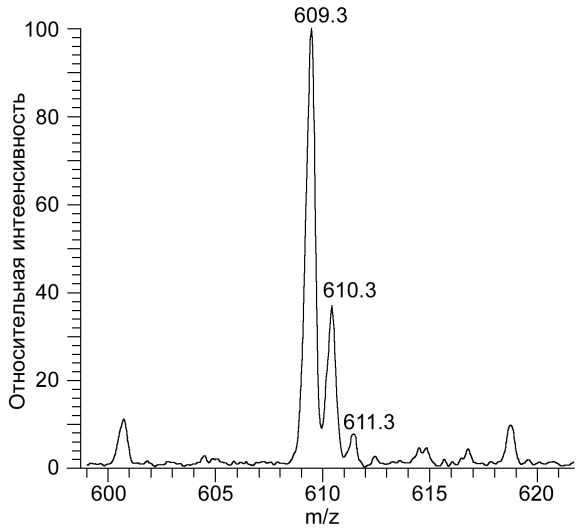

Fig. 10. ESI mass spectrum of the purified trypsin-derived Dend FP chromopeptide.

The mass of the original unmodified pentapeptide was calculated to be 645.3 Da. The comparison of the calculated and experimental masses (the difference is 37 Da) suggested that the Dend FP chromopeptide is a result of intramolecular cyclization reaction (the loss of H_2O molecule) and dehydrogenation reaction (the loss of H_2), similar to chromophore-forming reactions of GFP. Moreover, an additional difference of 17 Da was tentatively attributed to the loss of α-NH_2-group of His65 and additional double bond formation in the side chain of this aminoacid (-1H). All these assumptions were further checked by tandem mass-spectrometry and NMR.

MS/MS spectra of the Dend FP chromopeptide showed a number of daughter ions. Among them was a peak of m/z 609.3, which corresponds to the original chromopeptide molecular ion. Several positively charged ions corresponding to the fragmentation of His-Tyr-Gly-Asn-Arg pentapeptide were detected as well. Table 1 lists the assignments of MS/MS peaks, which are the result of collision-induced fragmentation of Dend FP chromopeptide main chain (according to the accepted nomenclature and due to the main chain definite cleavage sites, the peaks were assigned to the a^+, b+, c+ and x+, y+, z+ ions respectively).

Table 1. The MS/MS major peaks obtained after the collisional-induced fragmentation of Dend FP chromopeptide.

m/z (observed)	m/z (calculated)	Assignment	Relative amplitude
175,1	**175,1**	**y_1**	**0,6**
272,1	**272,1**	**z_2**	**1,2**
281,2	**281,1**	**c_2**	**1,8**
293,1	**293,1**	**a_3**	**1,1**
321,0	**321,1**	**b_3**	**3,5**
338,2	**338,1**	**c_3**	**1,2**
407,1	**407,1**	**a_4**	**5**
435,1	**435,1**	**b_4**	**10**
452,2	**452,2**	**c_4**	**23**

The obtained MS/MS data indicated that the Dend FP chromopeptide derives from both the photolytic intramolecular splitting of the bond between α-NH and α-carbon of His 65, and proteolytic cleavage of the polypeptide chain between Arg 69 and Val 70 with trypsin.

Task 9. Determination of the Dend FP chromophore fine structure by ^{1}H NMR.

For proton spin systems identification of the Dend FP chromopeptide we used homonuclear one- and two-dimentional TOCSY spectra. Analysis of the NMR data (Fig. 11A) allowed assignment of the proton signals. Five spin systems were identified in the spectrum – two of them corresponding to –NH-CαH(X)-$C_\beta H_2$-$C\gamma H_2$- $C_\delta H_2$-NH- (1) and – NH-CαH(X)-$C_\beta H_2$-CO- (2), and three spin systems corresponding to the unsaturated and aromatic bonds – (-CH=CH-)2 (3), -CH=CH- (4) и -CH=X-CH- (5). Spin systems 1 and 2 are due to aminoacid residues Arg (NH 8.03 ppm, $^{3}J_{NH\text{-}C\alpha H}$ 7.6 Hz; CαH 4.18 ppm; $C_\beta H_2$ 1.65 and 1.80 ppm; $C\gamma H_2$ 1.46 ppm; $C_\delta H_2$ 3.03 ppm and NεH 6.97 ppm, at 6.50 ppm the signal of guanidine group was identified) and Asn (NH 8.92 ppm, $^{3}J_{NH\text{-}C\alpha H}$ 6.6 Hz; CαH 4.7 ppm; $C_\beta H_2$ 2.79 and 2.90 ppm; the signals of the side chain amide protons were observed at 6.93 ppm and 7.63 ppm). Two doublets corresponding to the two proton units each (6.99 ppm and 8.12 ppm, ^{3}J 8.6 Hz, spin system 3) are due to δ- and ε-protons of the aromatic ring of Tyr 66 and a singlet at 7.24 ppm is due to Tyr 66 Cβ vinyl proton. The spin system 4 corresponds to the fragment -CαH=C_βH- (6.85 ppm and 7.86 ppm, ^{3}J 16.2 Hz) of the modified His 65 with trans orientation of the protons. The two doublets (J~0.4 Hz) one proton unit each at 7.71 ppm and 8.47 ppm are due to C4H and C2H signals of the modified His 65. The sixth spin system was observed at 20^{o}C – two signals, one proton unit each (J 17.7 Hz), which corresponds to $C_\alpha H_2$ of Gly 67. Therefore, the results of ^{1}H NMR are consistent with the structure III,which is shown in Fig. 11B.

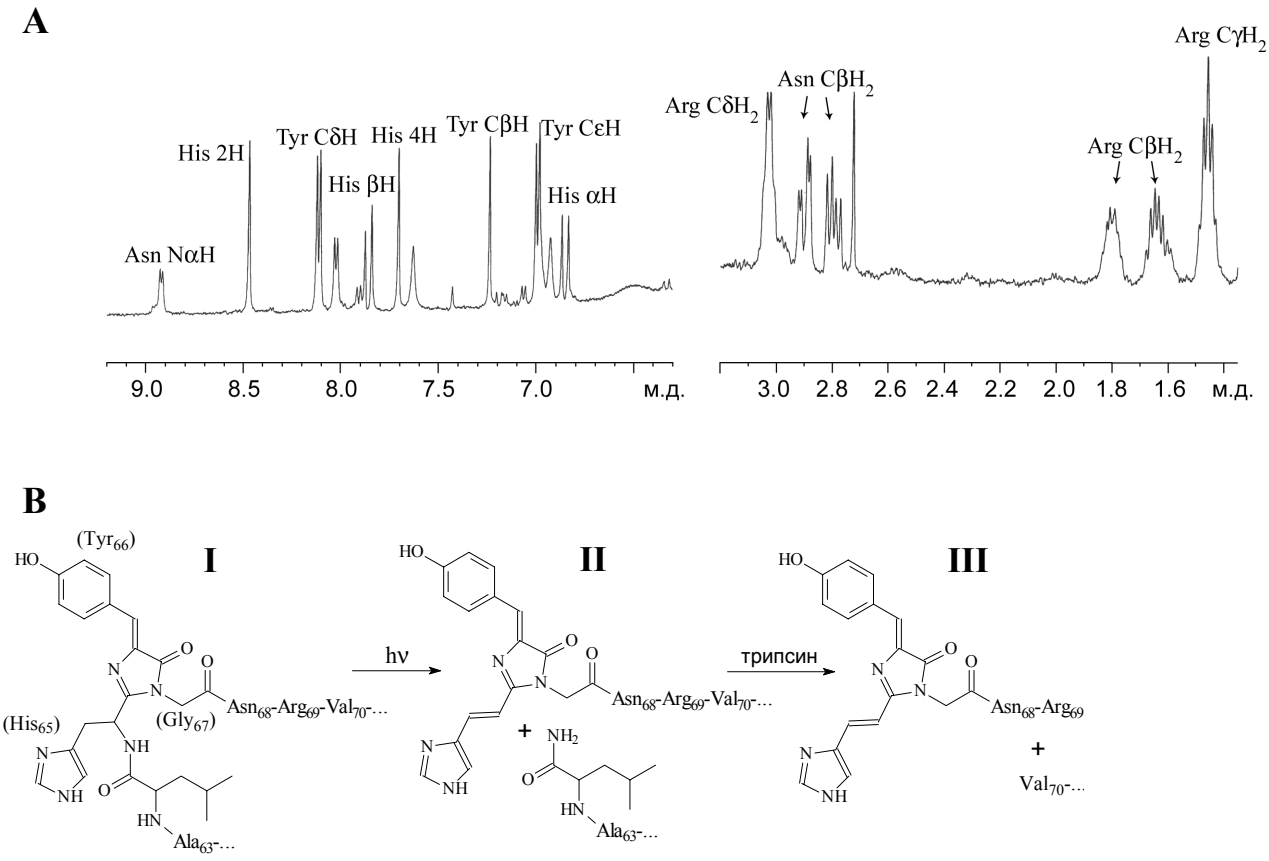

Fig. 11. The structure of the red form of the Dend FP chromophore. (A) ^{1}H NMR spectrum of the red form of the Dend FP chromopeptide in 10% D_2O, 30^{o}C, pH 4.0. (B) Summary scheme of the Dend FP chromopeptide formation, which is the result of photolytic cleavage of the polypeptide chain of the protein (green-to-red conversion, compound II) and proteolytic cleavage with trypsin (compound III**).**

Concluding remarks on the Dend FP chromophore structure.

In this part of work we have shown that a fluorescent protein from *Dendronephthya sp.* transforms from the green- to the red-emitting state by the pathway that differs greatly from the proteins of DsRed subfamily. Unlike green-to-red conversion of the DsRed chromophore, which seems to be an oxygen-dependent reaction, the Dend FP green-to-red transformation is a light dependent process, which does not require O_2. When our manuscript on this part of work was in preparation, Mizuno et al (Mizuno H. et al, (2003) Mol. Cell, **12**, 1051-1058) published their data on the chromophore structure of another fluorescent protein from the coral *Trachyphyllia geoffroyi* (Kaede). And although, unlike Dend FP dimeric structure, Kaede FP was shown to be an obligate tetramer, the formation pathways and the structures of the red chromophores were found to be the same for both proteins. Therefore, the results obtained for both proteins indicate that Kaede FP and Dend FP belong to the same subfamily of GFP-like proteins.

Task 6. Isolation of chromophore-bearing peptides from cgCP and gtCP.

Extensive digestion of cgCP with pepsin was performed at pH 2.8 overnight at enzyme to protein ratio of 1/30 at room temperature. Initially the resulting digest was fractionated using Bio-Gel P-2. Fractions absorbing at 380 nm were further subjected to HPLC separation on a

reverse-phase Ultrosphere ODS column (4.5x250 mm) equilibrated with 10 mM sodium phosphate buffer pH 4.0. Peptides were eluted with a linear gradient of acetonitrile. Figure 12A showes HPLC chromatogram of the separation of the P-2 chromopeptides fraction, monitored at 210nm and 380nm (in Fig 2A only 380nm track is shown). A major 380nm-absorbing chromopeptide was eluted at 24% of acetonitrile. Three minor chromopeptides were eluted at 23%, 26% and 29% of acetonitrile (Fig. 12A).

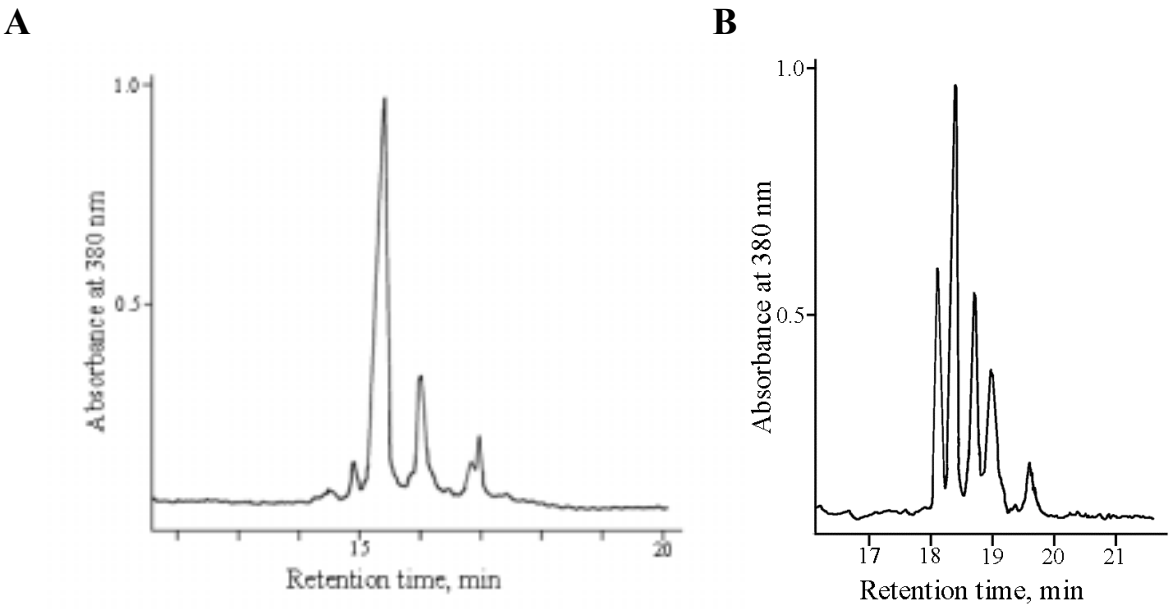

Fig. 12. HPLC purification of chromopeptides after extensive digestion by proteolytic enzymes. A. Isolation of 380nm-form of cgCP chromopeptide after extensive digestion with pepsin; **B.** Purification of chymotrypsin-derived gtCP chromopeptides.

Titration of the major chromopeptide eluted at 24% of acetonitrile gave rise to a characteristic 450 nm peak in absorption spectra at pH11.0, which shifted back to 380 nm when pH was adjusted to 3.0 (not shown). This pH-dependent transition was very similar to the behavior of a 380nm-form of denatured cgCP itself, suggesting that the terminal product of denaturation of cgCP and isolated chromopeptide include structurally identical chromophores.

A chromoprotein from *Goniopora tenuidens* was also subjected to extensive proteolytic digestion. Since our previous results indicated that gtCP contains structurally identical to DsRed chromophore, denaturation of gtCP was performed at basic conditions (pH 14.0) in order to minimize fragmentation of the protein. After denaturation (few seconds), a yellow protein sample was adjusted to pH 8.0 and a chymotrypsin was finally added (enzyme to protein ratio 1/30 w/w). A digestion was performed at room temperature for 4 hours. The total digest of gtCP was fractionated on a Bio-Gel P-2 column (1x30 cm) and a 380 nm-absorbing pool was further subjected to HPLC separation at the conditions similar to the described above for cgCP chromopeptide (Fig. 2B). One major gtCP chromopeptide peak was detected at 36% of linear acetonitrile gradient. Four minor gtCP chromopeptides were also isolated. Currently, we have isolated chromopeptides in quantity sufficient for structural studies.

Task 7. Aminoacid sequence determination of gtCP chromophore-bearing peptide.

A major gtCP chromophore-bearing peptide (36% of acetonitrile, see the previous report), derived from extensive chymotrypsin digestion was subjected to Edman degradation using Applied Biosystems 491 sequenator. Analysis of the degradation data revealed that SPQS- is the N-terminal aminoacid sequence of gtCP chromopeptide indicating that chymotrypsin cleaves the

peptide bond of gtCP between L 60 and S 61 (for the gtCP complete aminoacid sequence refer to the publication Gurskaya N.G. et al., (2001) *FEBS Lett.,* **507,** 16-20). Acid hydrolysis of gtCP chromopeptide followed by aminoacid analysis showed aminoacid content of 2.5 mol of serine, 1.9 mol of proline, 1.5 mol of glutamic acid, 0.3 mol of tyrosine, 1.5 mol of glycine, 0.9 mol of isoleucine, and 1.0 mol of phenylalanine. Carboxypeptidase treatment revealed that phenylalanine is a C-terminal aminoacid of the purified gtCP chromopeptide. Combined, the above data suggested that gtCP chromopeptide derives from an additional cleavage of the peptide bond between F 71 and T 72, yielding the fragment SPQSQYGSIPF.

Task 8. Mass-spectral characterization of the isolated gtCP chromopeptide.

One major and three minor HPLC-purified peptides absorbing at 380 nm were further analyzed by electrospray mass-spectrometry. Mass spectra of the major and all minor chromopeptides showed the same monoisotopic mass of 1187.4 Da (Fig. 13). These results confirmed the above findings that gtCP chymotrypsin-derived chromopeptide includes SPQSQYGSIPF aminoacid sequence. The mass of 1187.4 Da (calculated 1187.5 Da) also suggested that the gtCP chromophore derives from cyclization reaction (loss of H_2O) and two sites of dehydrogenation (loss of $2H_2$). If presumed a mature gtCP to contain a portion of molecules with GFP-like chromophore (one dehydrogenation site) then one would expect to see a noticeable increase of 1189 Da peak amplitude, just like as it was seen in DsRed chromopeptide mass spectra (Gross L.A. et al., (2000) PNAS, **97**, 11990-11995). The simulation mass profile of the gtCP chromopeptide (not shown), which accounts for the natural isotopic distribution, showed exactly the same relative abundance of the peak 1189 Da (24.14%) as observed in mass spectra. Thus, the above results are consistent with the existence of the gtCP chromophore preferably in the red state with two sites of dehydrogenation.

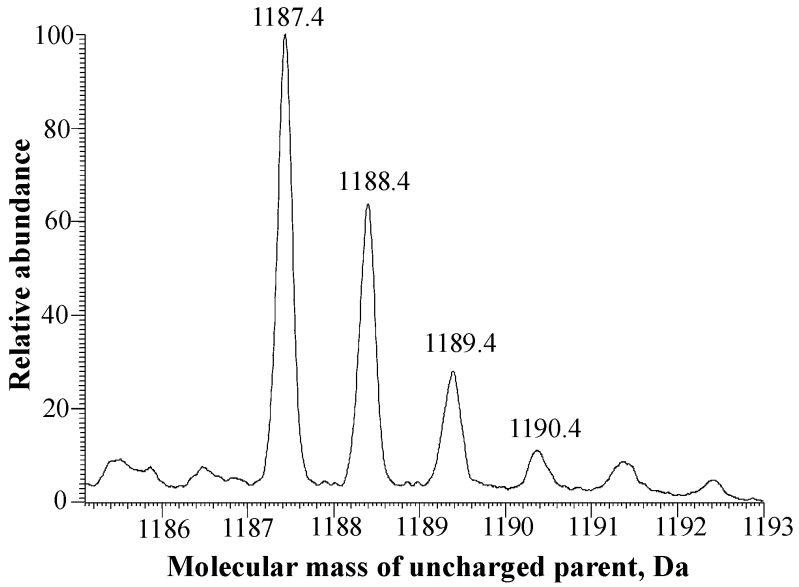

Fig. 13. Mass spectrum of the purified chymotrypsin-derived gtCP chromopeptide. Mass units shown are for uncharged parent species, deconvoluted from +1 and +2 species.

Further MS/MS fragmentation of the gtCP chromopeptide ion (parent mass 1187.4 Da) allowed positioning this additional dehydrogenation site between α-nitrogen and α-carbon of Gln 65 (Fig. 14). The most prominent peaks in the secondary MS resulted from the intramolecular cyclization reaction between α-carbon and δ-nitrogen of Gln 65 followed by splitting of the C=N bond (**II** and a complement fragment **I**, Fig. 14).

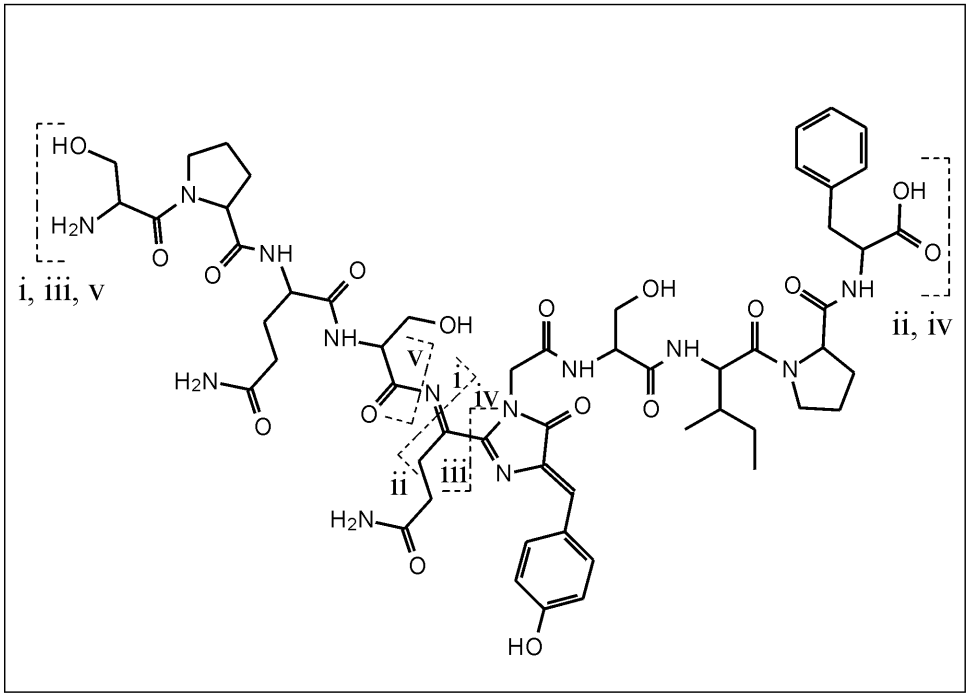

Fig. 14. Structure of gtCP chymotrypsin-derived chromopeptide. The most prominent MS/MS fragments are shown in the brackets

Similar fragmentation species were detected in MS/MS spectra of DsRed chromopeptide (Gross L.A. et. al., (2000) PNAS, **97**, 11990-11995). Many other daughter ions of gtCP chromopeptide were observed in the secondary mass spectrum, the most distinctive originating from fragmentation in the vicinity of acylimine C=N bond (**V**, **III** and **IV,** Table 2, Fig. 14).

Table 2. Distinctive peaks in MS/MS spectrum of the gtCP chromopeptide ion.

m/z (observed)	m/z (calculated)	Assignment	Relative amplitude
263.1	263.1	y_2	22
313.1	313.15	b_3	5
400.2	400.2	b_4 (**V**)	3
417.2	417.2	c_4 (**I**)	13
463.1	463.2	y_4	2
498.2	498.2	a_5 (**III**)	4
512.2	512.2	$(b_{10})^{2+}$	8
527.0	527.1	y_7b_9	1
691.2	691.3	x_6 (**IV**)	5
726.2	726.3	b_7	1
772.2	772.3	z_7-H (**II**)	30
813.3	813.3	b_8	1.5
926.3	926.4	b_9	100
1004.4	1004.4	y_9	13
1171.4	1171.5	z_{11}	31

Concluding remarks on gtCP chromophore structure.

In this part of work we have shown that a far-red chromoprotein from *Goniopora tenuidens* contains a chromophore of the same chemical structure as DsRed. Therefore, according to the above criteria, gtCP should be attributed to the DsRed subfamily of GFP-like proteins. Meanwhile, a recently published crystallographic structure of another GFP-like far-red protein from the sea anemone *Entacmaea quadricolor* (Petersen J. et al., JBC Papers in Press, August 8, 2003, Manuscript M307896200) revealed that this GFP-homologous pigment also includes a DsRed-like chromophore in which phenolic ring adopts *trans* conformation. Although we were unable to gain information relevant to gtCP chromophore conformation by the methods we used in this study, both published and our results suggest that a drastic chromophore structural reconstruction is not a prerequisite to the shift of spectra of GFP-like proteins to a far-red region. Thus, isomerization of the chromophore moiety and/or rearrangements in its interactions with surrounding aminoacid side chains seems to be sufficient in some cases for the color manifold of GFP-family proteins.

Task 7. Aminoacid sequence determination of cgCP chromophore-bearing peptide.

A major cgCP chromophore-bearing peptide (25% of acetonitrile, see report 5), derived from extensive pepsin digestion of the protein, was subjected to Edman degradation using Applied Biosystems model 491 Procise sequenator. Analysis of the degradation data revealed that SP- is the N-terminal aminoacid sequence of cgCP chromopeptide indicating that pepsin cleaves the peptide bond of cgCP between L 60 and S 61 (for the cgCP complete aminoacid sequence refer to the publication Gurskaya N.G. et al., *FEBS Lett.,* 2001, **507,** 16-20). Aminoacid analysis of the acid hydrolysed cgCP chromopeptide showed aminoacid content of 1.8 mol of serine, 0.9 mol of proline, 0.4 mol of tyrosine, 1.7 mol of glycine, 0.9 mol of alanine, 0.8 mol of lysin and 0.8 mol of threonine. Carboxypeptidase treatment revealed that Lys and Thr are the C-terminal aminoacids of the purified cgCP chromopeptide. Altogether, the above data suggested that cgCP chromopeptide derives from an additional cleavage of the peptide bond between T 70 and F 71, yielding the fragment SPCCAYGSKT.

Task 8. Mass-spectral characterization of the isolated cgCP chromopeptide.

The major cgCP chromophore-bearing peptide after HPLC purification was further analyzed by MALDI TOF mass-spectrometry.

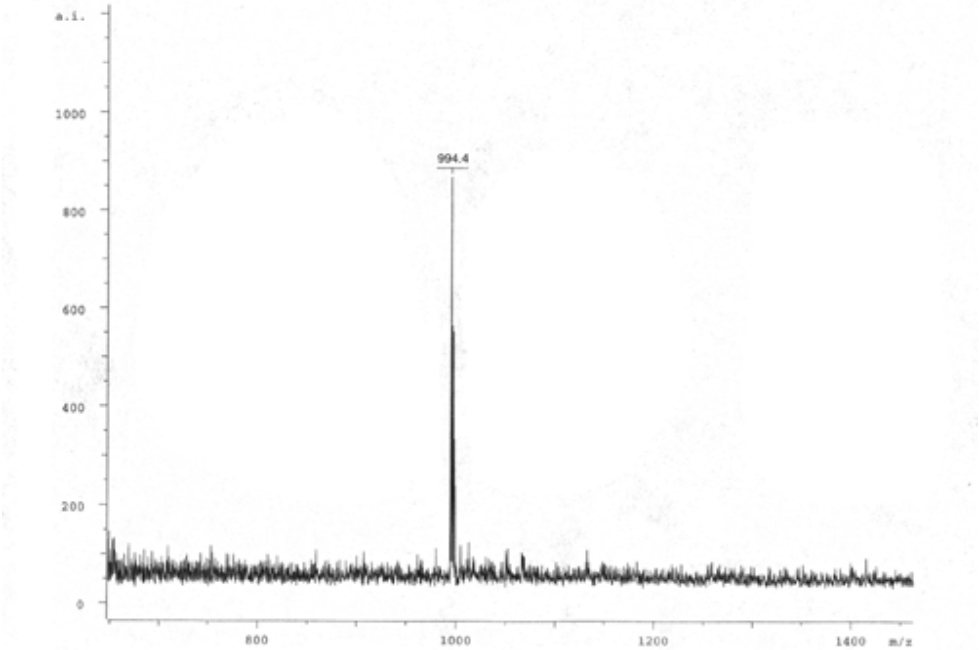

Fig. 15. Mass spectrum of the purified pepsin-derived cgCP chromopeptide

Mass spectra of the major cgCPchromopeptide yielded the molecular ion MH^+=994.4 (Fig. 15). This value corresponded to the mass of the chromopeptide 993.4 Da (calculated 993.4). The sequence SPCCAYGSKT was consistent with these mass spectral results, taking into account that the mass value of 993.4 Da is 22 Da lighter, than calculated (1015.4 Da) for the unmodified peptide with the same sequence. These results suggested that the cgCP chromophore derives from a cyclization reaction (loss of H_2O) and two sites of dehydrogenation (loss of $2H_2$), just as gtCP and DsRed chromophores do.

The MS/MS spectrum of collision-induced fragmentation of a cgCP chromopeptide ion yielded a number of fragments (Fig. 16). Among these fragments one can observe a peak with m/z of 994.4 corresponding to the parent peptide ion and many y^+ and b^+ ions, which are consistent with the masses of fragments after splitting of SPCCAYGSKT polypeptide backbone. Since cgCP contains one additional site of dehydrogenation, a special attention was set on peaks that derive from fragmentation in the vicinity of α-C-N bond of Ala 65. DsRed and gtCP was shown to contain C=N double bond at this position. Noteworthy, unlike DsRed and gtCP glutamine (Gln 65), the side chain of Ala 65 in cgCP would hardly to be expected to participate in the intramolecular cyclization reaction, which was shown to generate fragments in DsRed and gtCP secondary mass-spectra.

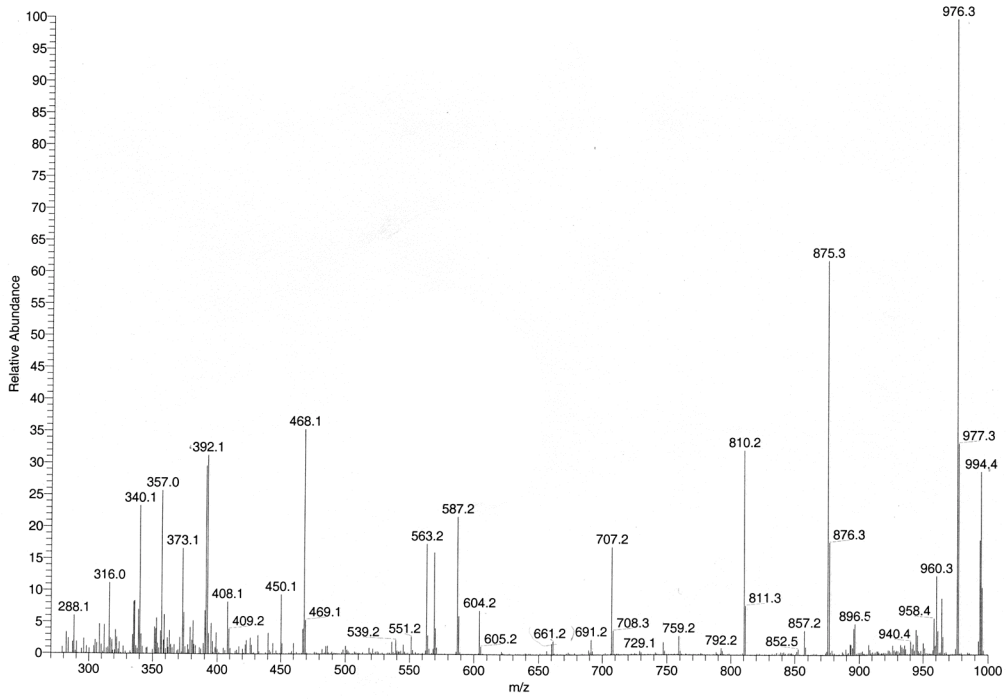

Fig. 16. ESI/MS/MS spectrum of the pepsin-derived cgCP chromopeptide.

Analysis of MS/MS data showed that both the fragment **IV** (Fig. 17) with m/z of 604.2 and the fragment **II** (m/z 587.2) still contain additionally dehydrogenated double bond. Conversely, the fragment **III** (m/z 563.2) contains only one site of dehydrogenation. Therefore, MS/MS data allowed tentative positioning of the additional dehydrogenation site of the cgCP chromopeptide between α- and β-carbons of Ala 65 (Fig. 17). This location of additional double bond differs from the site (acylimine C=N) found for the gtCP and DsRed chromophores and perhaps these data would explain, why cgCP upon harsh denaturing conditions fails to yield fragments in SDS/PAGE (see report 2).

Presently, we doubt that the native protein (cgCP) contains additional dehydrogenation at this position, because C=N double bond of the protein upon denaturation could undergo

tautomerization with the migration to Cα-Cβ. Therefore, we expect that further NMR and mutagenesis experiments would help to clarify the situation.

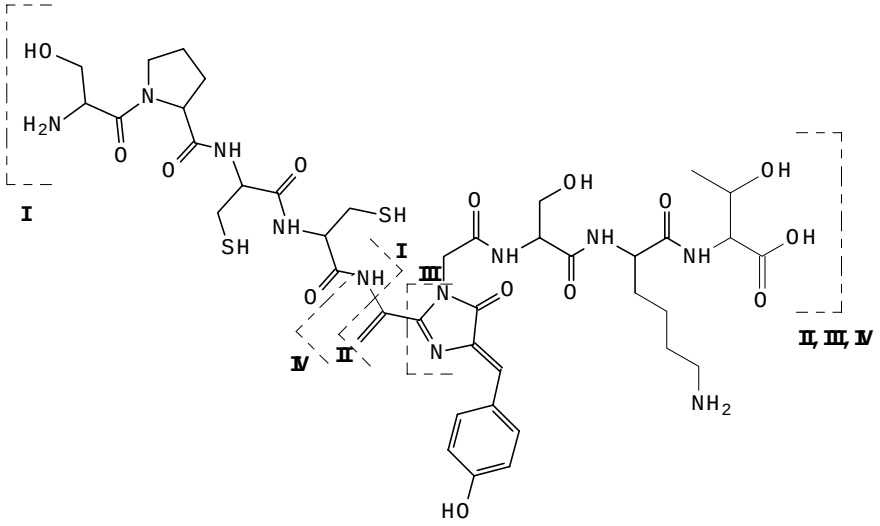

Fig. 17. Structure of the cgCP pepsin-derived chromopeptide.

Task 9. Blocking of isomerization to the side chain by A65G substitution.

To eliminate the possibility of isomerization of acylimine to enamide derivative, a point mutant, A65G, of cgCP was generated. Since glycine does not contain the side chain (Fig. 19), this kind of isomerization would not be expected in A65G mutant. Because wild type cgCP exhibits a characteristic absorbance at 570 nm, absorption maximum at this wavelength would indicate the formation of the "red" chromophore in A65G mutant in the only possible acylimine form. Absorbance around 500 nm would indicate the formation of an intermediate GFP-like form, lacking additional dehydrogenation. Moreover, these experiments would show if the side chain of aminoacid at the position 65 is critical for the red-shifting modification. Theoretically, one could expect additional dehydrogenation to proceed via intermediate enamide with the following isomerization to acylimine.

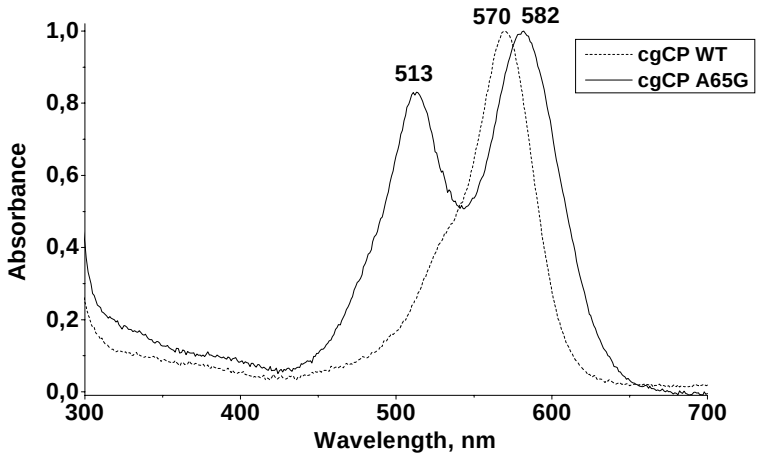

Fig. 18. Absorption spectra of cgCP and A65G mutant.

A65G mutant showed a characteristic 513 nm absorption maximum, corresponding to the intermediate GFP-like chromophore (Fig. 18) and this maximum further shifted to the 582 nm peak (the "red" chromophore) with time. Completely matured A65G mutant still contained substantial amount of the green form as judged by absorption spectra. Nevertheless, the maximum at 582 nm suggests that A65G mutant acquires the red-shifting modification in the form of acylimine (Fig. 19). The closely related maximum of wt cgCP suggests that the native wild type protein also contains additional dehydrogenation in the form of acylimine.

Since isomerization of additional double bond to the stable enamide derivative in A65G mutant is improbable, it is reasonable to expect the enhancement of A65G fragmentation as compared to the wild type protein. Indeed, SDS/PAGE indicated a noticeable increase of the extent of fragmentation of A65G (Fig. 21, lane 7) as compared to the wild type protein (Fig. 21, lane 3). Nevertheless, since A65G contains substantial amount of the green form, the extent of cleavage is less than 50% found for DsRed (Fig. 21, lane 1).

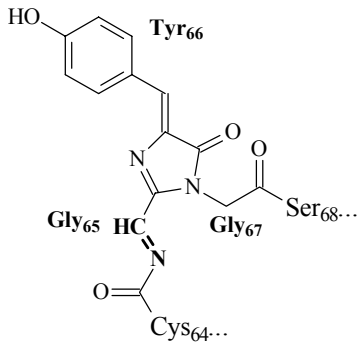

Fig. 19. Chromophore structure of the A65G mutant.

Summing up, the above results suggest that the bathochromic shift in A65G and in wt cgCP as well is induced by the extension of GFP-like chromophore by acylimine group. Earlier, according to the tandem mass-spectrometric data (report 7) we have presumed that denatured wt cgCP contains additional dehydrogenation in the side chain, between α- and β-carbons of Ala 65. Combined, these findings suggest that the red-to-green transition in cgCP absorption spectra upon denaturation corresponds to isomerization of the double bond to the side chain of Ala 65 and this isomerization would explain resistance to fragmentation of wt cgCP upon harsh denaturing conditions. Moreover, the above results indicate that the side chain of aminoacid at the 65th position is not prerequisite to the formation of the "red" chromophore and chromophore synthesis does not occur via enamide intermediate product.

The nature of the side chain of aminoacid 65 determines the extent of fragmentation.

Since unlike other proteins of DsRed subfamily wt cgCP proved to be resistant to fragmentation upon harsh denaturing conditions we decided to study the reactivity of acylimine C=N bond within cgCP chromophore. Sequence analysis shows that all the proteins susceptible to fragmentation contain Gln at 65th position (DsRed, gtCP, pocilloporin). It was important to check the influence of the side chain of the aminoacid 65 on the extent of fragmentation. Therefore, a single A65Q substitution was introduced to cgCP.

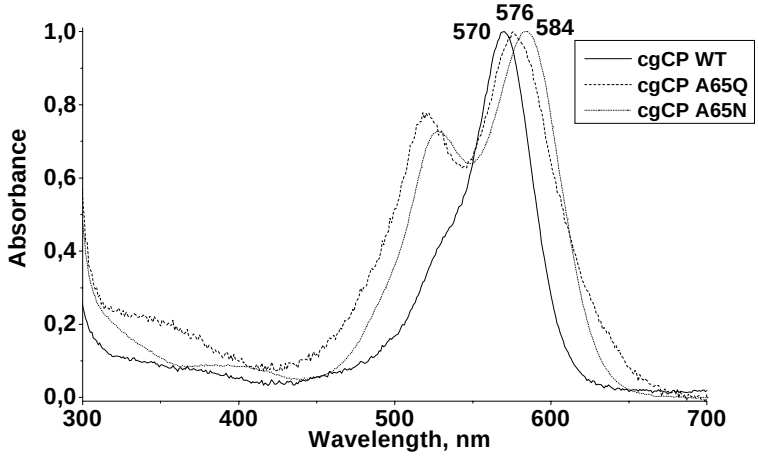

Fig. 20. Absorption spectra of wt cgCP, and A65Q, A65N mutants.

Mature A65Q mutant showed maximum absorption at 576 nm characteristic for the red form and, similarly to A65G, maximum at 520 nm corresponding to the immature GFP-like chromophore (Fig. 20).

A65Q mutant indeed showed enhanced fragmentation (Fig. 21, lane 5) as compared to wt cgCP (Fig. 21, lane 3). Assuming that substantial amount of A65Q exists in immature green form (Fig.

20), the red form seems to completely split into fragments. Therefore, the side chain of aminoacid 65 plays a crucial role in fragmentation of the protein.

One possible explanation of this phenomenon is a mechanism in which nucleophylic amido group of the side chain of Gln 65 attacks the carbon of acylimine group (Fig. 22). It is important that the side chain of Gln is able to form an intermediate cyclic structure. If this proposed mechanism is correct, then aminoacids unable to form intermediate cyclic structures would not favor fragmentation. To check this assumption a point mutant A65N was generated. The mature red form of A65N mutant absorbs maximally at 584 nm (Fig. 20), and like other mutants of cgCP contains noticeable amount of the green form (528 nm). But unlike A65Q, A65N mutant proved to be resistant to fragmentation (Fig. 21, lane 6). These results support the mechanism illustrated in Fig. 5. A highly homologous to cgCP protein, hcCP (82% identity), contains glutamic acid at the 65th position. Therefore we used this homologous protein as a model with A65E substitution. And though the glutamic acid is capable to form cyclic structures, hcCP does not split into fragments (Fig. 21, lane 4) that may be explained by reduced nucleophility of the side chain carboxy group, as compared to amido group.

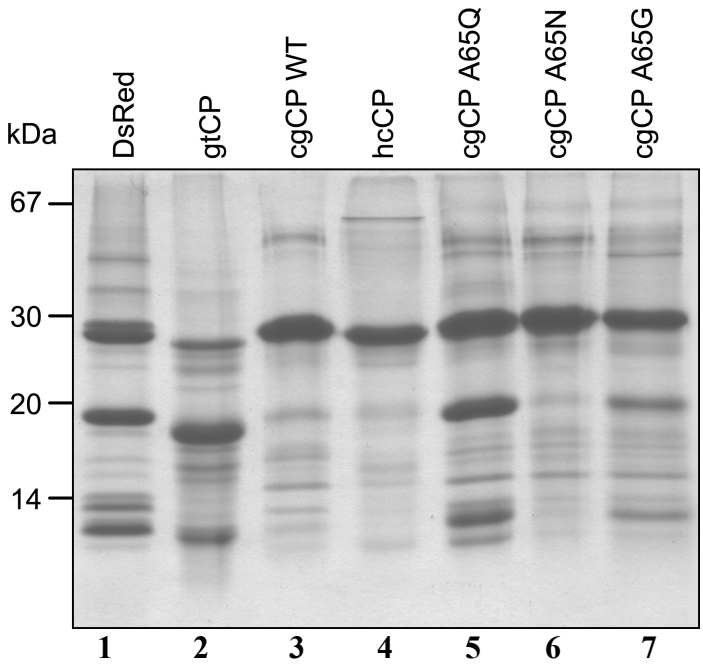

Fig. 21. Fragmentation of DsRed (1), gtCP (2), cgCP (3), hcCP (4) and cgCP mutants A65Q (5), A65N (6) and A65G (7) after boiling in 0.1 M HCl for 5 min.

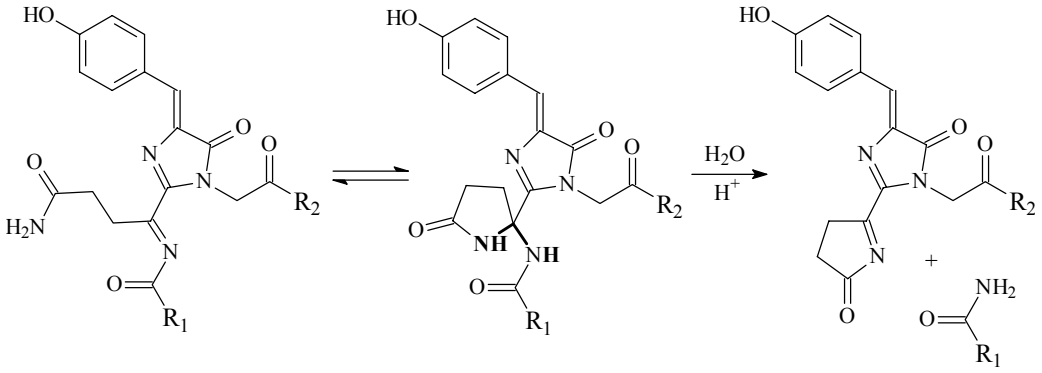

Fig. 22. The proposed mechanism of acylimine hydrolysis and fragmentation of the protein.

Task 9. The study of isomerization of cgCP chromophore by 1H NMR.

We have found earlier, that, similarly to DsRed and gtCP, cgCP chromophore undergoes spectral "red-to-green" transition upon mild denaturing conditions. Gross L.A. et al. attributed this transition to the addition of H_2O molecule across reactive acylimine C=N double bond in DsRed. Our tandem-mass-spectral studies indicated that it is isomerization of C=N bond that causes "red-to-green" transition of cgCP, but not addition of H_2O. Therefore, NMR studies of cgCP chromopeptide were aimed at elucidation of the structural basis of "red-to-green" transition.

The "green" form of cgCP was characterized by 1H NMR spectroscopy of the isolated cgCP chromopeptide. Initially, the exchangeable with the solvent amide protons were identified by spectral comparison of samples dissolved in H_2O or in D_2O. Afterwards, 2D homonuclear TOCSY and ROESY spectra were used for the identification of the amino acid 1H- spin systems. Altogether, nine spin systems were identified in 1H NMR spectra of the chromopeptide: H3N-CαH(X)-CβH2- (1), -N-CαH(X)-CβH2-CγH2-CδH2(N) (2), three spin systems -NH-CαH(X)-CβH2- (3, 4, 7), -CH=C-CH=CH- (5), -CαH2- (6), -NH-CαH(R)-CβH2-CγH2-CδH2-CεH2-N- (8), –NH-CαH(R)-CβHO-CH3 (9). Finally, each spin system was assigned to a specific amino acid residue of the chromopeptide (Table 3).

1H-signals assignment allowed elucidation of the structure of the chromopeptide. It is worth to dwell on the most prominent signals originating from the chromophore core structure. The signal of amide proton of Gly is absent from the NMR spectra of the chromopeptide, since Gly nitrogen is connected to three carbon atoms in imidazoline heterocycle of the chromophore center. The singlet signal of one proton unit from the modified Tyr CβH vinyl proton shows strong nuclear Overhauser effect (NOE) connectivity with the aromatic protons of the Tyr phenyl ring. The signals of amide and CαH protons of Tyr are absent from the NMR spectra of the chromopeptide, which is indicative of cyclization reaction at Nα and dehydrogenation at Cα of Tyr 66.

Table 3. Assignment of 1H-signals to the specific spin system

Amino Acid.*	Spin System	Assignment						
		NH	CαH2	CβH2	CγH2	CδH2	CεH2	NεH
Ser_{61}	1	-	4.22	3.90, 3.99				
Pro_{62}	2	-	4.37	1.96, 2.22	1.81, 1.96	3.58, 3.71		
Cys_{63}	3	8.36	4.42	2.89				
Cys_{64}	4	8.02	4.79	2.74, 2.91				
Ala_{65}		8.53	-					
Tyr_{66}	5	-	-	7.38		8.17	7.04	
Gly_{67}	6	-	4.72, 4.84					
Ser_{68}	7	8.59	4.53	3.89				
Lys_{69}	8	8.34	4.43	1.79, 1.91	1.46	1.70	3.00	7.50
Thr_{70}	9	7.91	4.22	4.27	1.16			

*Amino acids 65 – 67 form the chromophore center

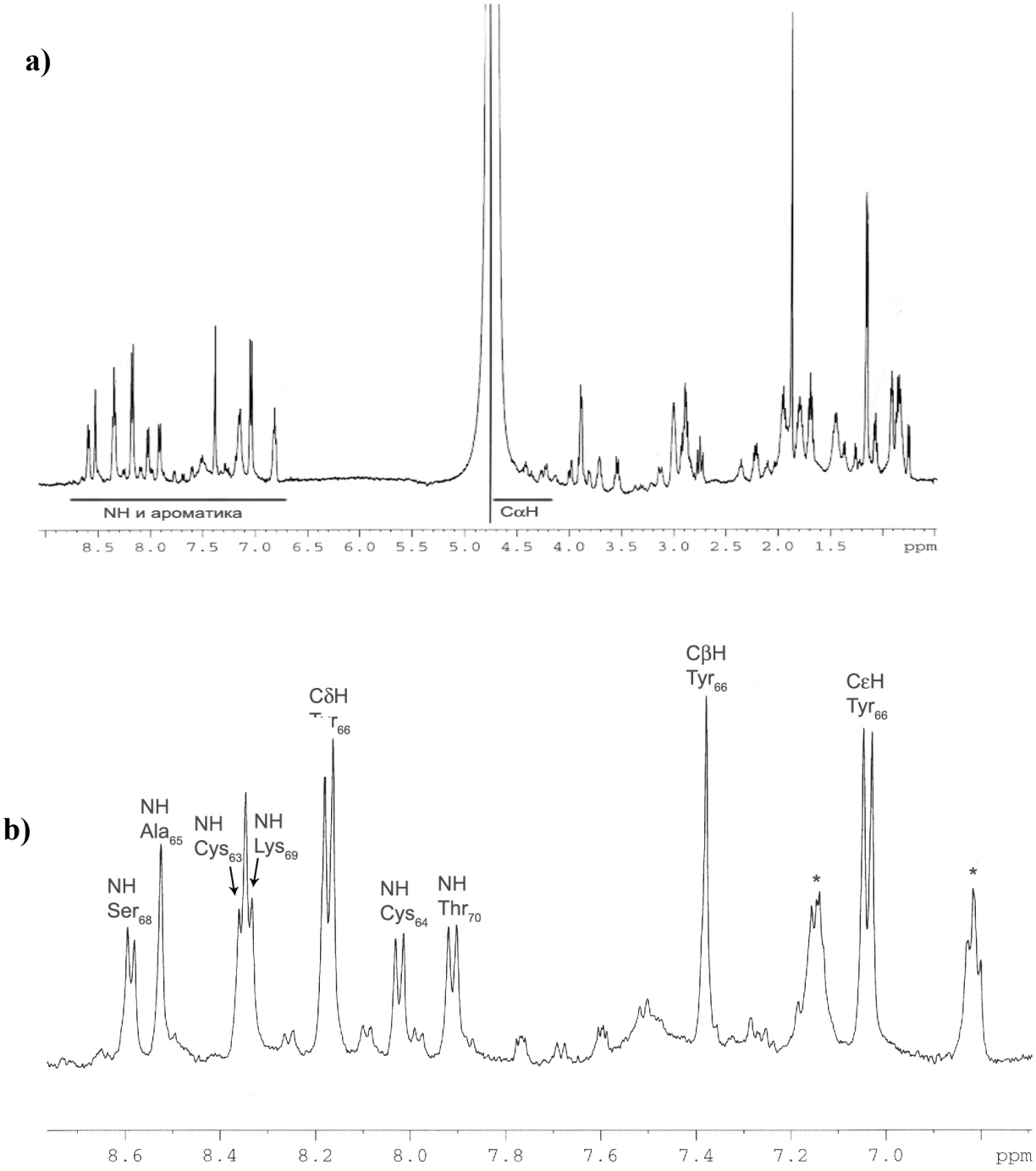

Fig. 23. *a) 1D-spectrum of the cgCP chromopeptide in 10% D2O at 30°C, b) NH and aromatic proton signals*

A singlet at 8.53 ppm (Fig. 23) corresponds to the amide proton of Ala 65, which excludes the presence of C=N double bond in the form of acylimine in the "green" form of cgCP chromopeptide. Moreover, the singlet implies the lack of CαH of Ala 65. Nevertheless, we could not obtain unequivocal data by 1H-NMR, as concerns the position of additional double bond isomerization, since we could not find the signals of CβH2 of Ala 65. Therefore, we expect that complementary studies of the "green" form of cgCP chromophore by 13C NMR will clarify the matter.

Task 9. The structure of the cgCP chromopeptide as studied by 13C- and 1H-NMR.

Initially, the experimental scheme was similar to that one we have used earlier (see report 11). First, the exchangeable with the solvent amide protons were identified by spectral comparison of samples dissolved in H_2O or in D_2O. After that, 2D homonuclear TOCSY and ROESY and heteronuclear 1H-13C-HMQC (Heteronucler Multiple Quantum Correlation Spectroscopy) and 1H-13C-HMBC (Heteronucler Multiple Bond Correlation Spectroscopy) spectra were used for the identification of the amino acid 1H-13C spin systems. Altogether, nine heteronuclear spin systems were identified and each heteronuclear spin system was assigned to a specific amino acid residue of the chromopeptide (Table 4).

Heteronuclear spin systems 1-4 and 8-10 were attributed to the corresponding unmodified amino acids, whereas the chemical shifts for the spin systems 5-7 differ from the typical ones of the unmodified Ala, Tyr and Gly respectively. The spin system 7, -CO-N(C=)-CH_2-CO, represents modified Gly67 and can be connected to Ser68 spin system 8 via the intervening Gly $^{13}C'$. The signal of amide proton at Gly67 is absent from the NMR spectra of the peptide and therefore must be connected to tree carbon atoms. The spin system 6, =X-C(=CH-C_6H_4-X)-CO (X represents N or O hetereatoms), represents modified Tyr66 connected to Gly67 spin system via Tyr $^{13}C'$. The spin system 5, CO-NH-C(CH3,X)-C=, represents modified Ala65. As it was observed before (see Report 11), 1H-NMR spectra show the presence of NH proton of Ala65 (a singlet signal of one proton unit at 8.53 ppm), which excludes the presence of C=N double bond in the form of acylimine in the "green" form of cgCP chromopeptide. Besids, this NH-singlet implies that Ala 65 lacks the alpha-carbon proton. Unlike the previous 1H-NMR experiment (Report 11), we observed a singlet signal (1.87 ppm) of three proton units, which corresponds to the CH_3-group of Ala65. This singlet signal from CH_3-protons shows strong nuclear Overhauser effect (NOE) connectivity with the NH-proton of Ala65. Moreover, the signal of CH_3-protons of Ala65 is shifted downfield from the normal position of Ala CH_3-protons. In addition, in 13C-NMR we observed the peak of Cα of Ala65 at 61.29 ppm, the value that differs from the usually observed for the unmodified Cα of Ala. These data may be indicative of the presence of hydroxy group at Cα of Ala65, as a result of water addition across the reactive acylimine C=N double bond. Therefore, the results obtained in the NMR experiments are consistent with the structure presented in the Fig. 24.

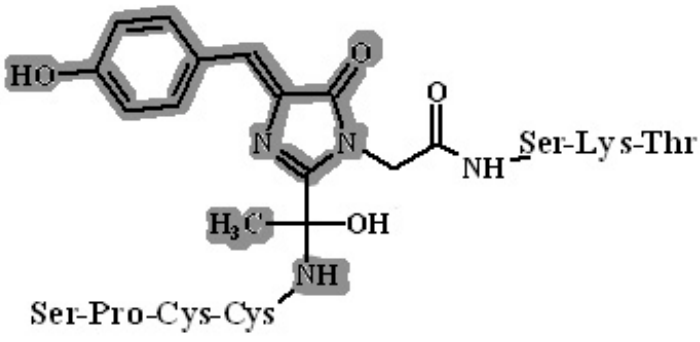

Fig. 24. The proposed structure of cgCP chromopeptide as deduced from NMR studies.

Table 4. Heteronuclear spin systems of the cgCP chromopeptide.

Residue (spin system)	ppm	Group
Ser61 (1)	53.23	$C^{\alpha}H$
	167.11	C′
	58.72	$C^{\beta}H_2$
Pro62 (2)	53.22	$C^{\alpha}H$
	174.20	C′
		$C^{\beta}H_2$
	25.21	$C^{\gamma}H_2$
	47.79	$C^{\delta}H_2$
Cys63 (3)	53.40	$C^{\alpha}H$
	172.13	C′
	31.13	$C^{\beta}H_2$
Cys64 (4)		$C^{\alpha}H$
	173.30	C′
	28.33	$C^{\beta}H_2$
Ala65 (5)	61.29	$C^{\alpha}H$
	162.02	C′
	23.96	$C^{\beta}H_3$
Tyr66 (6)		C^{α}
	173.57	C′
	133.20	$C^{\beta}H$
	126.51	C^{γ}
	135.75	$C^{\delta}H$
	116.28	$C^{\varepsilon}H$
	160.26	C^{Z}
Gly67 (7)		$C^{\alpha}H$
	169.61	C′
Ser68 (8)	55.11	$C^{\alpha}H$
	172.14	C′
	61.79	$C^{\beta}H_2$
Lys69 (9)	53.22	$C^{\alpha}H$
	173.76	C′
	24.18	$C^{\beta}H_2$
	21.64	$C^{\gamma}H_2$
	25.94	$C^{\delta}H_2$
	38.96	$C^{\varepsilon}H_2$
Thr70 (10)	59.54	$C^{\alpha}H$
	176.73	C′
	67.09	$C^{\beta}H_2$
	19.04	$C^{\gamma}H_3$

Intermediate and terminal spectral forms in maturation of red-shifted GFP-like proteins.

Current accepted mechanism of DsRed chromophore formation is the following. A GFP-like "green" chromophore (absorption at 480 nm, emission at 500 nm) is formed first, then, this green intermediate undergoes oxidation and turns into mature red chromophore (absorption at 558 nm, emission at 583 nm). This scheme was postulated on the basis of several observations. First, wild-type DsRed and many its mutants contain green emitting species. Second, in the course of protein maturation the green emission appears earlier than the red one and, then gradually decreases with the same rate as the red fluorescence grows. Third, the chemical structure of the red chromophore implies extension of GFP-like core.

However, our data suggest that this DsRed1 maturation scheme requires a revision. Because of an efficient energy transfer between green and red monomers within a DsRed1 tetramer, the decrease of the green fluorescence could be explained either by chemical transformation of the green chromophore into the red one or, alternatively, by an increase of the energy transfer to the later-maturing red chromophores. Absorption, but not emission, measurements would discriminate between these possibilities because they could reflect the true amount of each spectral form.

To measure changes in absorption curve during DsRed aging we purified *E. coli* expressed recombinant protein from culture at stage of active growth when the major part of the fluorescent protein exists in immature form. Then DsRed sample was left to mature in a cuvette and absorption spectra were measured over the time. The earliest measured DsRed sample demonstrated major absorption peak at 408 nm (B-form) together with smaller peak at 480 nm (G-form) and very small peak at 558 nm (R-form) (Fig. 25A, curve 1). Then, all three peaks increased for some period of time (Fig. 25A, curve 2). After this, amount of B-form gradually decreased up to zero at the end of maturation process (Fig. 25A, curves 3, 4). Peaks at 480 nm and 558 nm were found to growth over all time up to their maximal values.

Figure 25B shows the time course of B-, G-, and R-forms development normalized to their maximal values. These data allow us to conclude that R-form originates from the B-form, whereas the G-form is a dead end but not an intermediate as it was postulated earlier. This scheme explains the previously incomprehensible fact that mature wild-type DsRed as well as many its mutants contain the green-emitting chromophore that never converts into the red one.

Also, we monitored maturation of two DsRed mutants. The first mutant was "fluorescent timer" E5. This mutant showed very spectacular transformation of green into red fluorescence that led to mistaken conclusion about respective chemical conversion of green-emitting chromophore into the red one. As we expected, E5 mutant demonstrated practically the same absorption development as the wild type DsRed (not shown). Again, R-form apparently matured through intermediate B-form and amount of G-form never fell during maturation. Thus, we concluded that seeming change of fluorescence color is explained by very effective energy transfer from green-emitting to the later-maturing red-emitting monomers within E5 tetramers. Such energy migration was demonstrated for DsRed.

The second mutant was AG4 that possesses pure green fluorescence. Absorption spectrum for this mutant was peaked at 480 nm only over all maturation time. This protein contained neither B- nor R-forms that again demonstrated close correlation between them.

The data obtained allows to suggest the following scheme of maturation of DsRed and its mutant (Fig. 25C). Some spectrally undetectable initial form X can convert into either B-form or G-form. Then, B-form completely turns into R-form. So, final ratio between G- and R-forms depends on relative rates of reactions $X \rightarrow B$ and $X \rightarrow G$. Most probably, the B-form corresponds to neutral state of GFP-like chromophore. If so, dehydrogenation of Gln66 and formation of the "red" chromophore can occur only on protonated form of GFP-like intermediate. Apparently, deprotonated chromophore (G-form) can not turn into protonated state as it occurs in GFP due to absent of proton transfer pathway in DsRed.

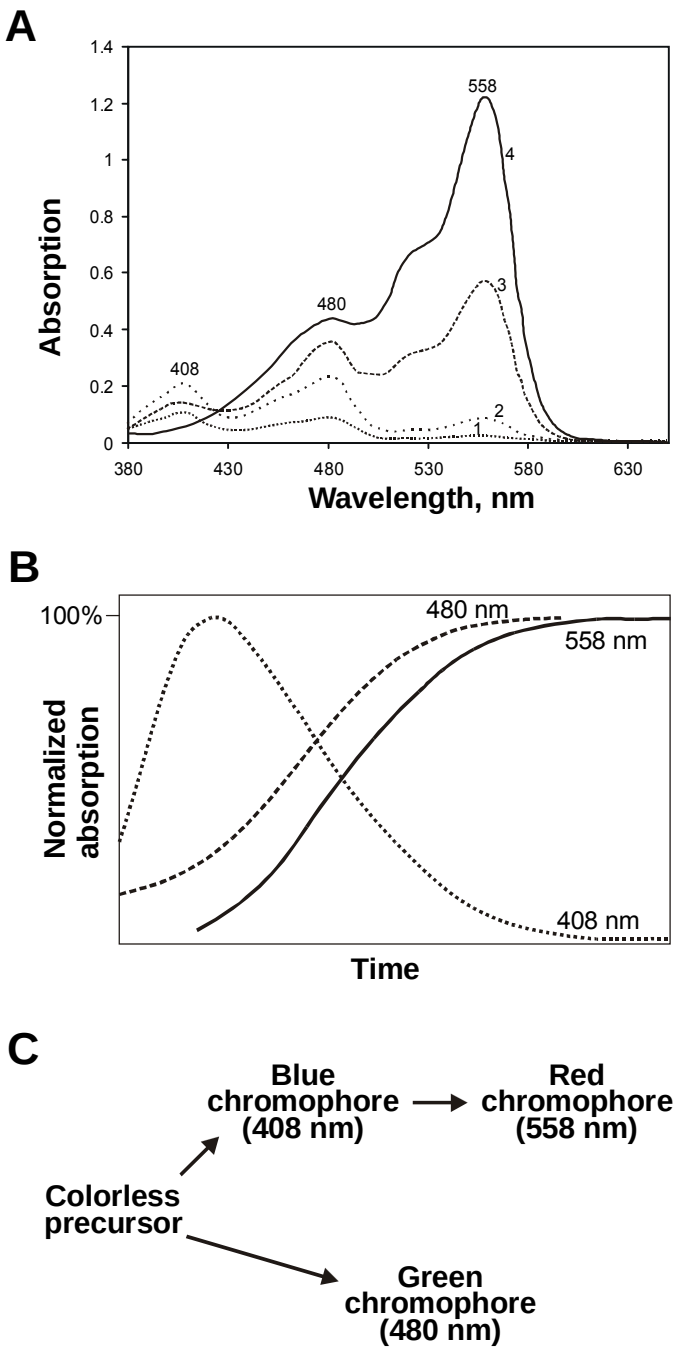

Fig. 25. Changes of absorption spectra during DsRed maturation. See text for details.

Then we analogously tested maturation process for three chromoproteins, cgCP, hcCP and asCP from *Condylactis gigantea, Heteractis crispa and Anemonia sulcata,* respectively. The earliest measured cgCP sample demonstrated major absorption peak at 400 nm (B-form) and smaller peak at 568 nm (R-form) (Fig. 26, curve 1). Then, both peaks increased for some period of time (Fig. 26, curve 2). After this, amount of B-form gradually decreased up to zero at the end of maturation process (Fig. 26, curves 3-5), while 568-nm peak increased up to its maximal value. So, 400-nm peak appeared to convert into 568-nm peak with isosbestic point at 465 nm.

hcCP showed practically the same maturation behavior as cgCP. Absorption peak at 400 nm gradually converted into 578-nm peak (data not shown).

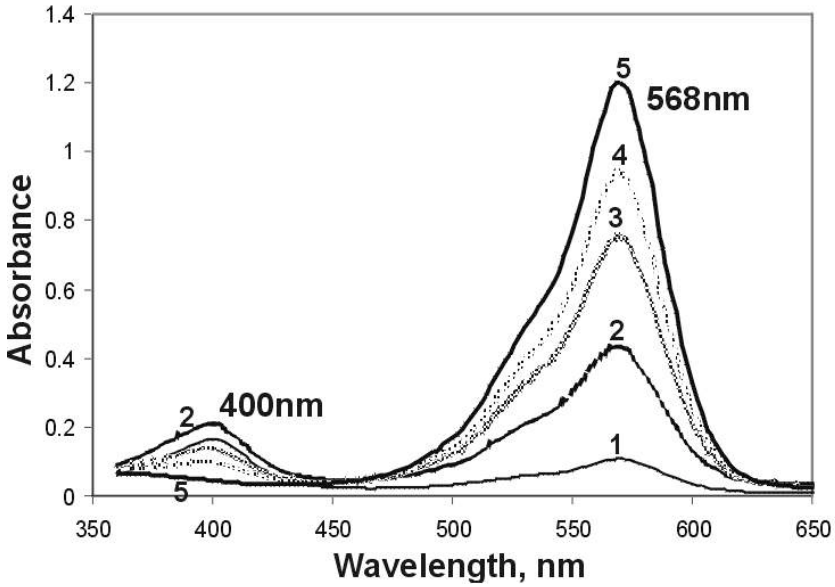

Fig. 26. Absorption spectra for maturing cgCP. Curves 1-5 represent consecutive stages of maturation with time.

Immature asCP possessed major absorption peak at 420 nm and a smaller peak at 568 nm. (Fig. 27, curve 1). In the course of maturation, amount 420-nm form decreased up to zero and peak of mature R-form (568 nm) increased (Fig. 27, curve 2-5). Isosbestic point at 560 nm was observed.

Thus, all three chromoproteins clearly demonstrated transformation of the intermediate B-form into the mature R-form. In contrast to DsRed, no spectral form absorbing at 480-500 nm (G-form) was detected in these proteins. These data showed the maturation of red chromophores through blue-absorbing intermediate is probably a universal pathway in coral red fluorescent proteins and chromoproteins.

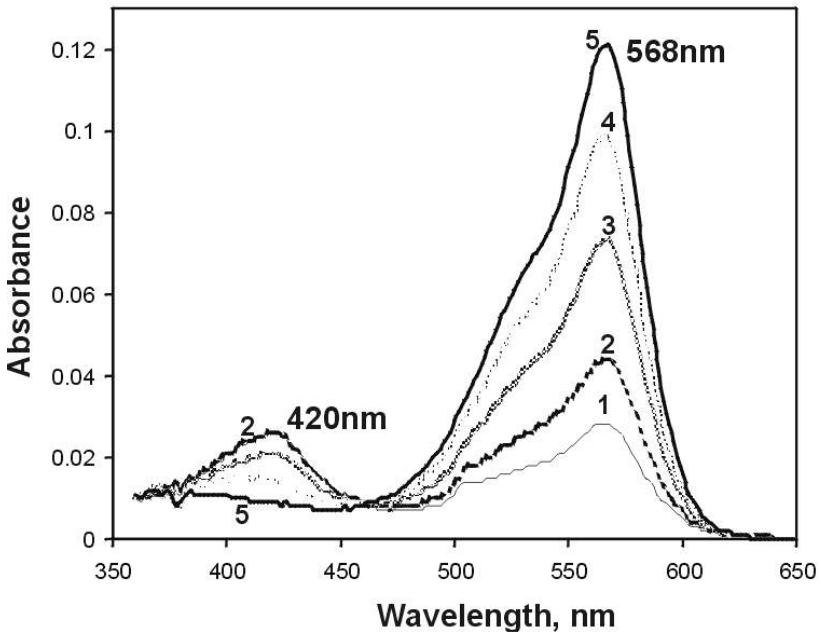

Fig. 27. Absorption spectra for maturing asCP. Curves 1-5 represent consecutive stages of maturation with time.

Then we tested fluorescence of these spectral forms during maturation of DsRed-E5 ("Fluorescent timer") mutant. Fluorescence spectra for G- and R-forms were published by Terskikh and coauthors (Terskikh et al., "Fluorescent timer": protein that changes color with time. Science 2000, 290, 1585-1588), so we focused on detection of the B-form.

To detect intermediate B-form we purified *E. coli* expressed recombinant DsRed-E5 protein from culture at stage of active growth when the major part of the fluorescent protein exists in immature form. Then DsRed-E5 sample was left to mature in a cuvette and emission spectra were measured over the time. Excitation at 400 nm produced a weak but clearly detectable peak of blue fluorescence at 450 nm. In the course of protein maturation 450-nm peak decreased up to zero (Fig. 28).

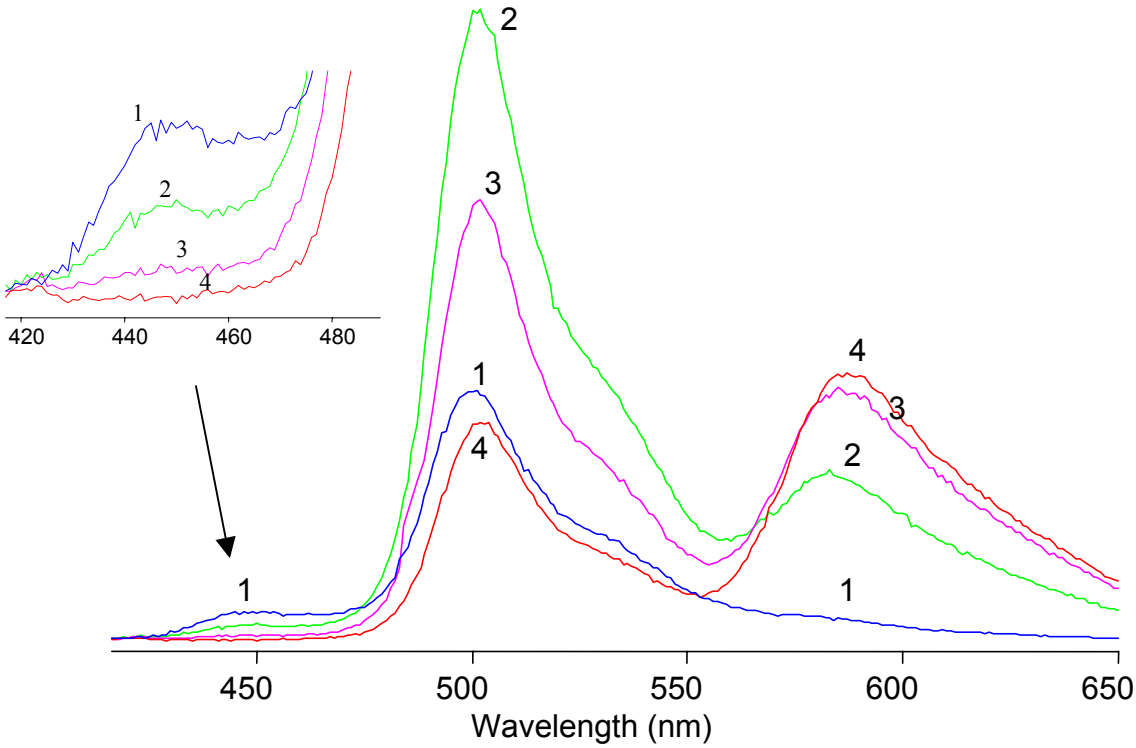

Figure 28. Changes of DsRed-E5 emission spectrum (excitation at 400 nm) during its maturation. Curves 1-4 represent consecutive stages of maturation with time.

Due to pronounced changes of relative intensities of green (500 nm) and red (583 nm) fluorescence during DsRed-E5 maturation this protein was found to be an excellent tool for visualization of up- and down-regulation of promoter activity as well as of "age" of target proteins and organelles (Teskikh et al., Science 2000, 290, 1585-1588; Duncan et al., Nature 2003, 422, 176-180). Apparently, analysis of DsRed-E5 blue fluorescence would visualize very early stages of its maturation. The following experiments demonstrated utility of blue fluorescence detection in living cells.

Three-color "fluorescent timer" in living mammalian cells. To study possibility to detect fluorescence of the B-form in mammalian cells we have expressed DsRed-E5 fluorescent timer in HEK293 cells. To synchronize induction, DsRed-E5 was expressed under Tet-On inducible system, and standard DAPI, FITC and Cy3 filter sets were used. Distinct blue and green fluorescence was visible and detectable by CCD camera after 6-8 hours, whereas cells with all three colors, blue, green and red, have appeared only 12-14 hours after the start of induction

(Fig. 29). The ability to detect B-form by standard methods extends fluorescence timer features to twice shorter times after reporter induction than in case of detection G- and R-forms, and from three to four sequentially changeable color hues: blue, white, yellow and red (Fig. 29, overlay). This will allow detection of fast promoter activities and distinguishing more populations of aging organelles or cells *in vivo*.

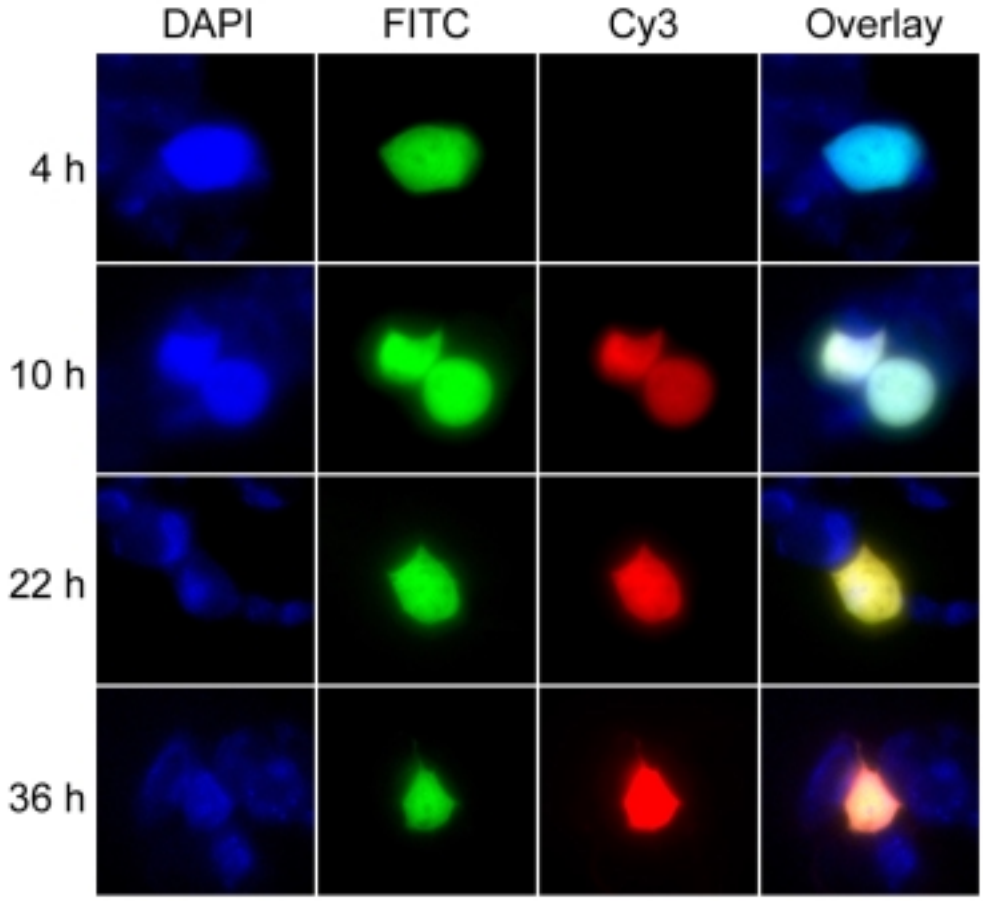

Figure 29. Pulse-chase induction of Tet-On regulated DsRed-E5 in human HEK293 cells. Fluorescence images in the respective wavelength channels (from the left to the right: DAPI, FITC, and Cy3), and their overlay (the most right column) of the representative living cells are shown. Tet-On induction was performed for 4 hours, the time values at the left indicate the times after the start of Tet-On induction.

Light sensitivity of the B-form. We found a sensitivity of the B-form to the illuminating light. Illumination of cells expressing DsRed-E5 at DAPI channel resulted in a detectable decrease of the blue and the respective increase in the red fluorescence. We studied this light-induced B->R transition for DsRed1 in detail. First, an action spectrum of this transition was determined, in which we measured the relative increase in the red fluorescence of overnight grown *E. coli* colonies expressing DsRed1 after irradiation at the different wavelengths (Fig. 30A). We found that two wavelengths, 410 and 380 nm, are the most effective for the light-induced conversion. These wavelengths were consistent with decomposition of the B-form absorption peak onto Gaussian peaks at 408 nm and 382 nm. Finally, we studied the dependence of the light-induced conversion from a light intensity at the fixed wavelength (Fig. 30B). The dependence was linear suggesting that this transition is a one-photon process.

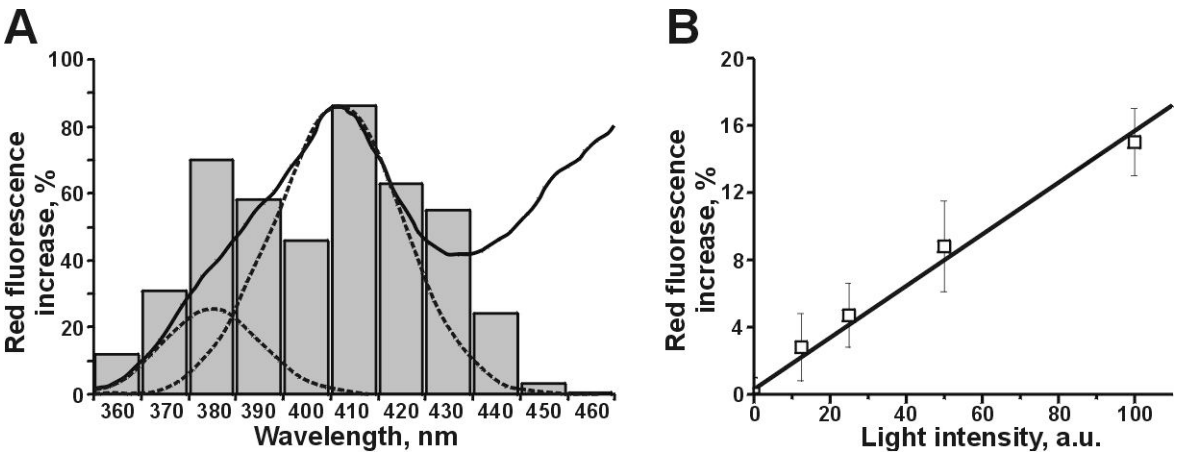

Fig. 30. Light-induced conversion of DsRed. (**A**) Action spectrum is presented as the histogram showing relative increase of the DsRed red fluorescence after its irradiation with light of the defined wavelengths. The fluorescence before irradiation was taken for 100%. Immature DsRed1 absorption spectrum (solid line) and its Gaussian decomposition (dashed lines) are shown for comparison. (**B**) Linear dependence of the increase in the DsRed red fluorescence from the light intensity.

Light-induced fluorescence acquisition in vivo. This light-induced effect can be exploited to accelerate the fluorescence acquisition for DsRed variants in living cells. Indeed, at early stages of DsRed1 expression in *E. coli* we were able to increase the red fluorescence signal 3.5-4.5-fold by 2-3 min intense irradiation with 405 nm using a fluorescent stereomicroscope (not shown). To further verify this feature, mammalian cells expressing DsRed2 18 h after transfection were irradiated using the DAPI filter and 100x objective and then imaged in Cy3 channel. The red fluorescence intensity increased 1.6-2.0-fold and reached a plateau within 90-120 sec for different cells (Fig. 31). The pre-exposure to far-UV-Violet light resulted in the visible increase of the red fluorescence without affecting cellular morphology. Thus, the maturation of commonly used DsRed and DsRed2 markers could be significantly accelerated. Soon after the expression starts the red fluorescence is weak, one can easily enhance the fluorescence signal several-fold by brief irradiation of expressing cells through the conventional DAPI channel.

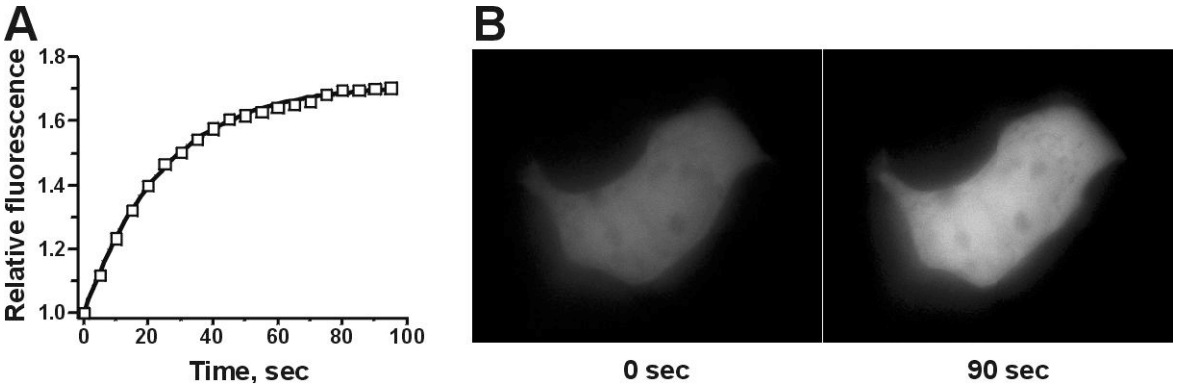

Fig. 31. Light-induced acceleration of the DsRed2 maturation in living human HEK293 cells. The time-course for the red fluorescence growth is shown (**A**). The total intensity of the cell before the light-treatment was taken for 1. The image of the representative cell before (0 sec) and 90 sec after the irradiation through DAPI filter (**B**).

Investigation of violet and blue pigments from scyfoid jellyfish *Rhizostoma pulmo*

To extend the spectrum of available red-shifted GFP-like proteins with potentially novel red and far-red absorbing chromophores we started to search for new GFP homologs. The main goal of this branch of our project is discovery of distant homologs of Anthozoa fluorescent proteins and following determination of their choromophore structures.

To date, GFP-like proteins were found in two classes of Coelenteratae: Hydrozoa and Anthozoa. It would be very interesting from both practical and scientific points of view to identify GFP homologs in class Scyphozoa. With that end in view, we caught several specimens of jellyfish *Rhizostoma pulmo* (class Scyphozoa) from the Black Sea. This jellyfish is non-fluorescent but possesses bright coloration: its umbrella border and ends of oral arms are rich violet while oral arms are light blue. Our working hypothesis is that coloration of this medusae is possibly determined by non-fluorescent GFP-like chromoproteins as it was demonstrated for corals. If so, they should contain red-shifted chromophores with absorption maximum at about 600 nm (violet-blue color).

Primary characterization of the violet and blue pigments was made on crude protein extracts from corresponding parts of the jellyfish. Extraction was made by placing of the medusae pieces in phosphate buffered saline (PBS) and storing for several days at 4°C. As a result, significant amount of coloring agents transferred from tissues into solution. Thus, both pigments were found to be well soluble. Their absorption spectra were similar to each other but blue pigment displayed red-shifted absorption maximum (580 nm for the violet and 600 nm for the blue pigments, respectively) (Fig. 32). Both pigments were non-fluorescent.

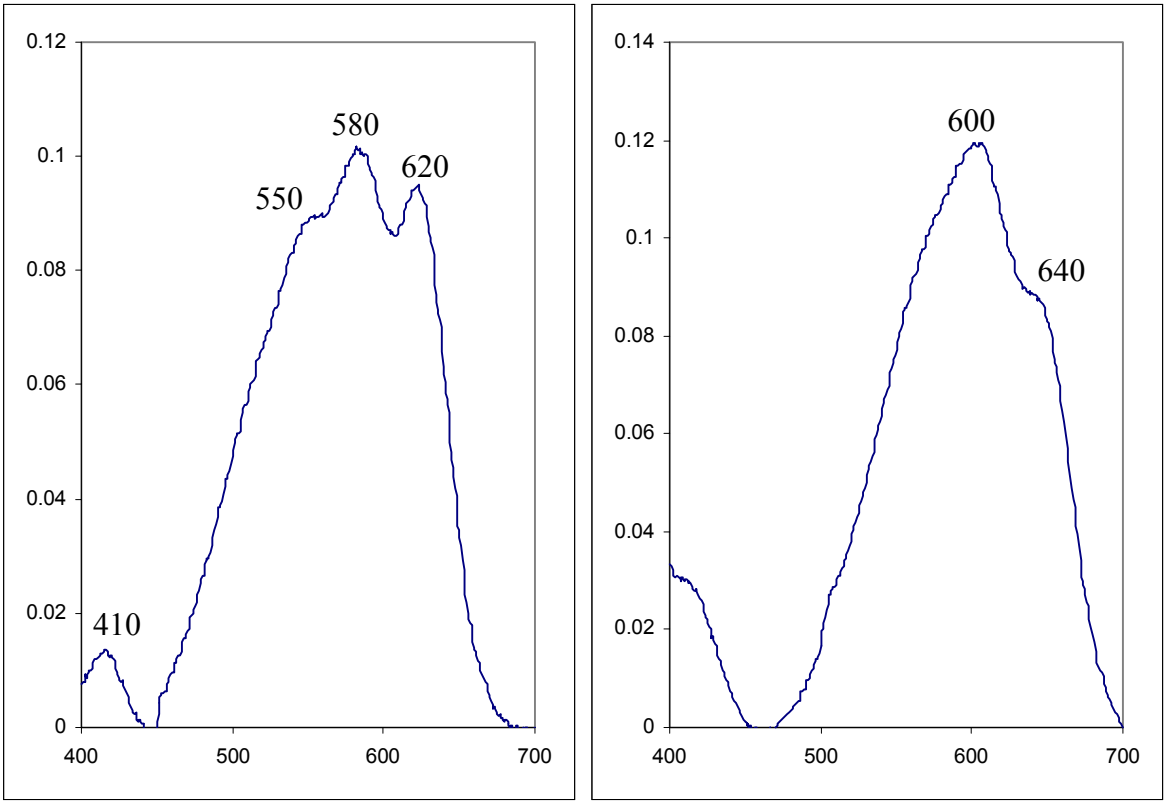

Figure 32. Absorption spectra for the violet (left) and blue (right) pigments from jellyfish *Rhizostoma*.

To investigate a chemical nature of the pigments we made several simple tests. First, we performed phenol extraction of the colored samples. This treatment resulted in complete loss of the blue and violet coloration. Since phenol denatures proteins we concluded that the blue and violet pigments are protein-based.

Then, we found that treatment with chloroform did not change the color of aqueous phase. It is well known that chloroform is not so strong denaturing agent as phenol and some proteins with a firm tertiary structure remain stable in the presence of chloroform. In particular, GFP-like proteins can not be denatured by chloroform.

The most widespread pigments in nature are carotinoids and carotinoproteins (non-covalent complexes of carotinoids with specific proteins). Carotinoids are usually yellow, orange or red but in complexes with proteins they can give practically all colors including violet-blue hues. A specific test for carotinoid-based pigments is their effective extraction from tissues by cold acetone. Also, after denaturation of carotinoproteins their absorption changes to color characteristic of corresponding free carotinoid. For instance, blue cuticle of lobster becomes red after heating.

These tests demonstrated that the pigments from *Rhizostoma* do not contain carotinoids. First, acetone did not extract any colored agents from the jellyfish tissues. Second, the violet and blue samples after heating became colorless but not orange-red as it should be in the case of carotinoproteins.

Then we analyzed the violet sample (it contained more intensive coloration than the blue extract) by common protein SDS-PAGE (Fig. 33). The heated sample was found to contain a major band of 28 kDa. In the non-heated sample this protein band migrated as 30 kDa and was colored. It should be noted that GFP-like proteins also save their coloration in conditions of SDS-PAGE if samples are not heated before loading.

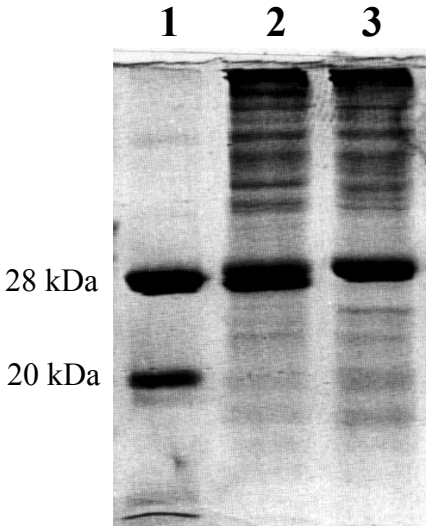

Figure 33. Protein gel-electrophoresis of the violet extract from umbrella border of *Rhizostoma*. Lane 1 - purified DsRed (heated sample). Lane 2 - heated jellyfish extract. Lane 3 - non-heated jellyfish extract (the 30-kDa protein band was colored before Coomassie staining).

In order to clone genes encoded colored proteins from *Rhizostoma pulmo* we used direct partial sequencing of purified protein of interest for following PCR with degenerative primer(s) corresponding to the known amino acid sequence. To purify violet protein we used precipitation with ammonium sulfate. It was found that in saturated $(NH_4)_2SO_4$ this pigment precipitated into floated violet flakes. Gel-electrophoresis of these dissolved flakes showed that it contained almost pure violet protein. The colored protein band after SDS-PAGE of non-heated sample was

transferred onto PVDF membrane, cut and used as a template for automatic protein sequencing. The following confident 20 amino acid sequence was obtained: SAVPAKMVQLLREKVPLNIE.

To clone cDNA for violet pigment protein we designed degenerate primer (5'-GCT GTT CCN GCN AA(A/G) ATG-3') corresponding to fragment AVPAKM of the known 20 amino acid sequence SAVPAKMVQLLREKVPLNIE. This primer together with oligo-dT-containing primer were used for amplification of 3' fragment of specific cDNA. After cloning and sequencing of this fragment, we used 5'-RACE procedure to obtain 5' flank of this cDNA. As a result, sequence of whole coding region for *Rhizostoma* violet protein (RVP) was obtained.

Unexpectedly for us, RVP did not belong to the family of GFP-like proteins. NCBI BLAST analysis revealed two clearly detectable domains within RVP: so called Frizzled cystein rich domain and Kringle domain (Fig. 34).

```
        10         20         30         40         50         60         70
MAKAIVAMLLLFFTNVEMTISSAVPAKMVQLLREKVPLNIEFCRLAMGYSETAKINFMQQTNQSLVQQDR

        80         90        100        110        120        130        140
LFKALLTLSKFGCSELTEAYTCATYAPPVIAPYGALPPCRSLCKNVKGNCDALTTAMAKHLANGECKMTT

       150        160        170        180        190        200        210
EGGDYRGKVSQTFDGVKCQAWDTQEPHRHSVTAKTHPNDGLESNYCRNPDGESKGPWCYTTSGRRWDYCA

       220        230        240        250        260
VPKCKVQFYCNYFPEPSENQGCVDYTYNRKEAKLELLVRGNPRARIDPWAIPEY
```

Fig. 34. Amino acid sequence of the *Rhizostoma* violet protein. Signal peptide are shaded in gray. The fragment revealed earlier by protein sequencing is underlined. The Frizzled- and Kringle-related domains are shaded in blue and yellow, respectively. Note that Kringle domain is incut into the Frizzled domain.

The Frizzled CRD (cysteine rich domain) is conserved in diverse proteins including several receptor tyrosine kinases. In *Drosophila*, members of the Frizzled family of tissue-polarity genes encode proteins that appear to function as cell-surface receptors for Wnts. The Frizzled genes belong to the seven transmembrane class of receptors and have in their extracellular region a cysteine-rich domain that has been implicated as the Wnt binding domain. The structure of this domain is known and is composed mainly of alpha helices. This domain contains ten conserved cysteines that form five disulphide bridges.

Kringles are autonomous structural domains, found throughout the blood clotting and fibrinolytic proteins. Kringle domains are believed to play a role in binding mediators (e.g., membranes, other proteins or phospholipids), and in the regulation of proteolytic activity. Kringle domains are characterised by a triple loop, 3-disulphide bridge structure, whose conformation is defined by a number of hydrogen bonds and small pieces of anti-parallel beta-sheet. They are found in a varying number of copies, in some serine proteases and ROR-like receptors. Plasminogen-like kringles possess affinity for free lysine and lysine-containing peptides.

Conclusions. We found a novel type of protein-based pigments consisting of Kringle domain inserted into Frizzled domain. Association of these domains with coloration was never shown although many Kringle- and especially Frizzled-containing proteins are well studied.

The main question to be solved further is the nature of chromogenic group in *Rhizostoma* pigments. To solve the chromophore chemical structure we need to collect sufficient amounts of *Rhizostoma* specimens, purify pigment protein, digest it with proteases and isolate pure chromogenic group. Finally, its chemical structure can be determined by mass spectrometry and NMR.

Synthesis and properties of the chromophore of asFP595 chromoprotein

Chemical synthesis of natural compounds makes it possible to obtain large amounts of a pure substance of known structure, to characterize it in detail and to support the results of prior investigation into the chemical structure. Investigation of a synthetic GFP chromophore clarified details of its spectral behavior. However, structural studies of the chromophores found within red-shifted GFP-like proteins are complicated by the instability of the isolated compounds in solution. Chemical modifications can also occur during mass spectral analysis or intense X-ray irradiation. Ideally one should use a combination of independent approaches to arrive at a reliable conclusion about the chromophore structure within the native protein. Chemical synthesis appeared to be a useful method to study the chromophores of GFP-like proteins that allow to check results obtained by other methods.

Except for a model GFP chromophore, no other natural chromophores from GFP-like proteins have been synthesized to date. The only work on this matter described synthesis of a compound similar to but not identical to the chromophore within DsRed (He et al., Org. Lett. 4, 1523-1526.). Here we present the first synthetic chromophore for a red-shifted protein of GFP family.We deveploped a high-efficient pathway for synthesis of the chromophore for the purple nonfluorescent chromoprotein asFP595, based on the proposed chromophore structure resulting from high resolution crystallographic studies of the protein (data from laboratory of Prof. S. James Remington, Oregon University, USA).

Synthesis. A general approach to the 4-arylidene-5-imidazolones includes Ehrlenmeyer azlactone formation followed by aminolysis with the primary amine of choice and subsequent cyclization in alkaline conditions. We used this approach to synthesize 2-ethyl-4-(p-hydroxybenzylidene)-1-methyl-5-imidazolone (**3**) (Scheme 1). Oxidation of **3** with 1 equivalent of selenium dioxide in dioxane gave 2-acetyl-4-(p-hydroxybenzylidene)-1-methyl-5-imidazolone (**4**) in 60% yield. ^{1}H and ^{13}C NMR spectra of **4** are fully consistent with proposed structure. In particular, peak at 192.8 ppm in ^{13}C NMR spectrum refers to key carbonyl group in the acetyl substituent.

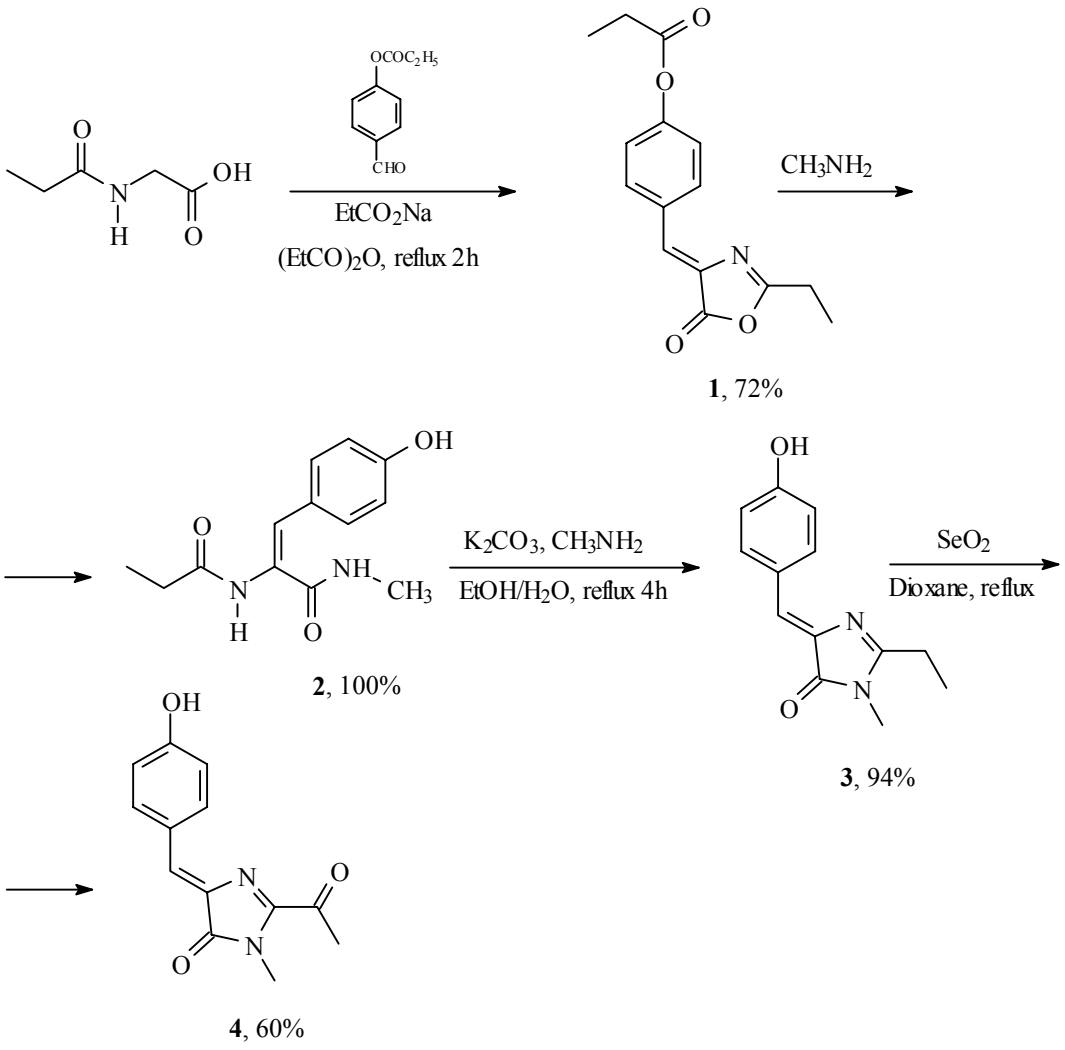

Scheme 1. Synthesis of asFP595 chromophore.

Spectral properties of the model asFP595 chromophore. The absorption spectrum of compound **4**, the proposed model chromophore, demonstrated clear dependence on pH. In water solution at acidic pH the absorption maximum was at 418 nm, while at neutral and slightly basic pH 520 nm. Interconversions of these forms by pH titration were found to be completely reversible with pKa 7.1 (Figure 35A). We attribute this to the equilibrium between the neutral and anionic forms (structures **4a** and **4b** respectively, Figure 35A) of the chromophore, similar to the well-characterized behavior of the GFP chromophore.

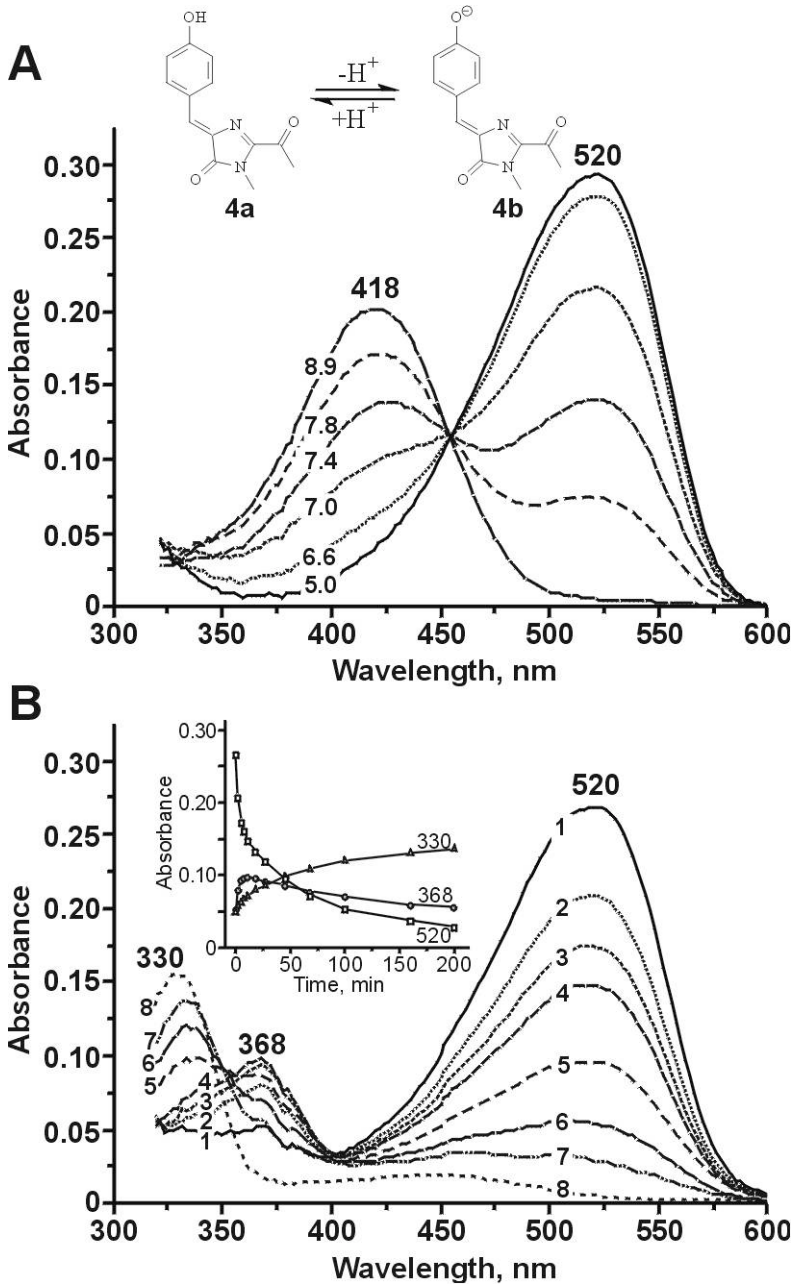

Figure 35. (A) Spectrophotometric titration of chromophore **4** water solution. (B) Degradation of the chromophore in 10 mM aqueous NaOH. Curves 1-8 corresponds to 0, 2, 5, 11, 45, 100, 200 and 1200 min of incubation, respectively. Inset shows absorption changes at 334, 368 and 520 nm during the first 200 min.

At pH 11.0 or higher the model chromophore underwent slow degradation (half-life about 20 min at pH 12) into unidentified products with absorption at 368 and 330 nm (Figure 35B). Acidification at different time-points during this process resulted in appearance of different amounts of neutral form **4a** corresponding to the current amount of anionic form **4b**.

The nature of the solvent had a strong impact on absorption maximum of the anionic form **4b** of the chromophore (Table 5). Absorption maximum wavelength of the anionic form **4b** increased in the range water-ethanol-isopropanol-dimethylformamide. We attribute this behavior to solvent protonic acidity rather than solvent polarity as stated by Niwa and coworkers (*Proc. Natl. Acad. Sci. USA 93*, 13617-13622). We propose that hydrogen bonds between the negatively charged chromophore phenolic oxygen and its surroundings (protein or solvent shell)

substantially raise the energy required for excitation, causing the behavior of the anionic chromophore to more closely resemble that of the neutral protonated form **4a**.

Table 5. Absorption characteristics of the chromophore in different solvents. Spectra for neutral and anionic forms were measured in 10 mM HCl and 10 mM NaOH respectively.

Solvent	Absorption max, nm (extinction coefficient, $M^{-1}cm^{-1}$)	
	Neutral form	Anionic form
Water	418 (35,000)	520 (47,000)
Ethanol	425 (40,000)	542 (72,000)
2-Propanol	428 (39,000)	552 (73,000)
DMF	422 (38,000)	572 (87,000)

The most red-shifted absorption maximum at 572 nm was found in DMF, which is very close to the absorption maximum of the asFP595 protein (568 nm) (Figure 36A). DMF solution of the chromophore form **4b** (pH 8.3) showed weak red fluorescence at 603 nm (Figure 36B). We estimated chromophore fluorescence quantum yield at room temperature to be $2.1*10^{-3}$. The wild type asFP595 protein demonstrated fluorescence at the same wavelength, but remarkably, the quantum yield was tenfold lower ($2.2*10^{-4}$). The reverse is normally true for fluorescent proteins. For example, the GFP chromophore is essentially non-fluorescent in solution at room temperature but possesses very high quantum yield within the native protein. For the free chromophore, it is widely held that photoisomerization is responsible for nonradiative energy dissipation, whereas in GFP the protein shell restricts chromophore motion. The structural basis for the lack of fluorescence in asFP595 and other GFP-like chromoproteins is presently unclear. However, our data suggest that the protein shell in asFP595 actively favors the non-radiative processes, making the chromophore even less fluorescent than in solution.

In DMF, the anionic form **4b** demonstrated spectral properties that are very close to those of the native asFP595 in terms of shape and peak positions in absorption, excitation and emission spectra. Thus we believe this form represents a chromophore state within asFP595.

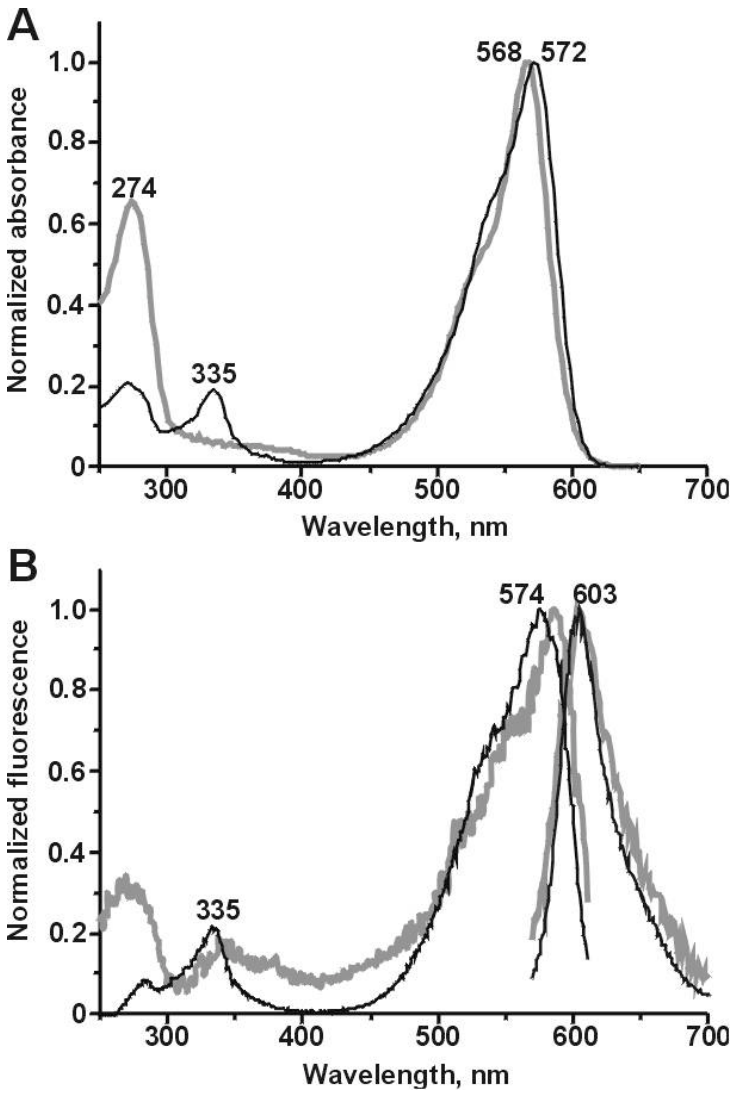

Figure 36. Comparison of absorption (A) and excitation-emission (B) spectra of the chromophore **4b** in DMF (thin black lines) and native asFP595 (thick gray lines). Within each pair of lines the emission spectrum is the one at longer wavelengths.

List of published papers

1. Martynov V.I., Maksimov B.I., Martynova N.Y., Pakhomov A.A., Gurskaya N.G., Lukyanov S.A. A purple-blue chromoprotein from Goniopora tenuidens belongs to the DsRed subfamily of GFP-like proteins. *J. Biol. Chem*., 2003, **278**, 46288-46292.

Abstract: A number of recently cloned chromoproteins homologous to the green fluorescent protein show a substantial bathochromic shift in absorption spectra. Compared with red fluorescent protein from Discosoma sp. (DsRed), mutants of these so-called far-red proteins exhibit a clear red shift in emission spectra as well. Here we report that a far-red chromoprotein from Goniopora tenuidens (gtCP) contains a chromophore of the same chemical structure as DsRed. Denaturation kinetics of both DsRed and gtCP under acidic conditions indicates that the red form of the chromophore (absorption maximum at 436 nm) converts to the GFP-like form (384 nm) by a one-stage reaction. Upon neutralization, the 436-nm form of gtCP, but not the 384-nm form, renaturates instantly, implying that the former includes a chromophore in its intact state. gtCP represents a single-chain protein and, upon harsh denaturing conditions, shows three major bands in SDS/PAGE, two of which apparently result from hydrolysis of an acylimine C=N bond. Instead of having absorption maxima at 384 nm and 450 nm, which are characteristic for a GFP-like chromophore, fragmented gtCP shows a different spectrum, which presumably corresponds to a 2-keto derivative of imidazolidinone. Mass spectra of the chromophore-containing peptide from gtCP reveal an additional loss of 2 Da relative to the GFP-like chromophore. Tandem mass spectrometry of the chromopeptide shows that an additional bond is dehydrogenated in gtCP at the same position as in DsRed. Altogether, these data suggest that gtCP belongs to the same subfamily as DsRed (in the classification of GFP-like proteins based on the chromophore structure type).

2. Pakhomov A.A., Martynova N.Y., Gurskaya N.G., Balashova T.A., Martynov V.I.. Photoconversion of the chromophore of a fluorescent protein from Dendronephthya sp. *Biochemistry (Moscow)* 2004, **69,** 901-908.

Abstract: A green fluorescent protein from the coral Dendronephthya sp. (Dend FP) is characterized by an irreversible light-dependent conversion to a red-emitting form. The molecular basis of this phenomenon was studied in the present work. Upon UV-irradiation at 366 nm, the absorption maximum of the protein shifted from 494 nm (the green form) to 557 nm (the red form). Concurrently, in the fluorescence spectra the emission maximum shifted from 508 to 575 nm. The green form of native Dend FP was shown to be a dimer, and the oligomerization state of the protein did not change during its conversion to the red form. By contrast, UV-irradiation caused significant intramolecular changes. Unlike the green form, which migrates in SDS-polyacrylamide gels as a single band corresponding to a full-length 28-kD protein, the red form of Dend FP migrated as two fragments of 18- and 10-kD. To determine the chemical basis of these events, the denatured red form of Dend FP was subjected to proteolysis with trypsin. From the resulting hydrolyzate, a chromophore-containing peptide was isolated by HPLC. The structure of the chromophore from the Dend FP red form was established by methods of ESI, tandem mass spectrometry (ESI/MS/MS), and NMR-spectroscopy. The findings suggest that the light-dependent conversion of Dend FP is caused by generation of an additional double bond in the side chain of His65 and a resulting extension of the conjugated system of the green form chromophore. Thus, classified by the chromophore structure, Dend FP should be referred to the Kaede subfamily of GFP-like proteins.

3. Verkhusha VV, Lukyanov KA. The molecular properties and applications of Anthozoa fluorescent proteins and chromoproteins. *Nature Biotechnol.* 2004, **22**, 289-296. Review.

Abstract: The green fluorescent protein (GFP) from the jellyfish Aequorea victoria and its fluorescent homologs from Anthozoa corals have become invaluable tools for in vivo imaging of cells and tissues. Despite spectral and chromophore diversity, about 100 cloned members of the GFP-like protein family possess common structural, biochemical and photophysical features. Anthozoa GFP-like proteins are available in colors and properties unlike those of A. victoria GFP variants and thus provide powerful new fluorophores for molecular labeling and intracellular detection. Although Anthozoa GFP-like proteins provide some advantages over GFP, they also have certain drawbacks, such as obligate oligomerization and slow or incomplete fluorescence maturation. In the past few years, effective approaches for eliminating some of these limitations have been described. In addition, several Anthozoa GFP-like proteins have been developed into novel imaging agents, such as monomeric red and dimeric far-red fluorescent proteins, fluorescent timers and photoconvertible fluorescent labels. Future studies on the structure of this diverse set of proteins will further enhance their use in animal tissues and as intracellular biosensors.

4. Verkhusha VV, Chudakov DM, Gurskaya NG, Lukyanov S, Lukyanov KA. Common pathway for the red chromophore formation in fluorescent proteins and chromoproteins. *Chem Biol.* 2004, **11**, 845-854.

Abstract: The mechanism of the chromophore maturation in members of the green fluorescent protein (GFP) family such as DsRed and other red fluorescent and chromoproteins was analyzed. The analysis indicates that the red chromophore results from a chemical transformation of the protonated form of the GFP-like chromophore, not from the anionic form, which appears to be a dead-end product. The data suggest a rational strategy to achieve the complete red chromophore maturation utilizing substitutions to favor the formation of the neutral phenol in GFP-like chromophore. Our approach to detect the neutral chromophore form expands the application of fluorescent timer proteins to faster promoter activities and more spectrally distinguishable fluorescent colors. Light sensitivity found in the DsRed neutral form, resulting in its instant transformation to the mature red chromophore, could be exploited to accelerate the fluorescence acquisition.

5. Bulina ME, Lukyanov KA, Yampolsky IV, Chudakov DM, Staroverov DB, Shcheglov AS, Gurskaya NG, Lukyanov S. New class of blue animal pigments based on Frizzled and Kringle protein domains. *J Biol Chem.* 2004, **279**, 43367-43370.

Abstract: The nature of coloration in many marine animals remains poorly investigated. Here we studied the blue pigment of a scyfoid jellyfish Rhizostoma pulmo and determined it to be a soluble extracellular 30-kDa chromoprotein with a complex absorption spectrum peaking at 420, 588, and 624 nm. Furthermore, we cloned the corresponding cDNA and confirmed its identity by immunoblotting and mass spectrometry experiments. The chromoprotein, named rpulFKz1, consists of two domains, a Frizzled cysteine-rich domain and a Kringle domain, inserted into one another. Generally, Frizzleds are members of a basic Wnt signal transduction pathway investigated intensely with regard to development and cancerogenesis. Kringles are autonomous structural domains found throughout the blood clotting and fibrinolytic proteins. Neither Frizzled and Kringle domains association with any type of coloration nor Kringle intrusion into Frizzled sequence was ever observed. Thus, rpulFKz1 represents a new class of animal pigments, whose chromogenic group remains undetermined. The striking homology between a chromoprotein and

members of the signal transduction pathway provides a novel node in the evolution track of growth factor-mediated morphogenesis compounds.

6. Yampolsky I.V., Remington S.J., Martynov V.I., Potapov V.K., Lukyanov S., Lukyanov K.A. Synthesis and properties of the chromophore of the chromoprotein asFP595 from Anemonia sulcata. *Biochemistry,* 2005, **44**, 5788-5793.

Abstract: A model compound for the chromophore within the purple non-fluorescent GFP-like chromoprotein asFP595 was synthesized. The postulated structure of the chromophore, 2-acetyl-4-(p-hydroxybenzylidene)-1-methyl-5-imidazolone, was taken from the high resolution crystal structure analysis of intact asFP595 (accompanying paper Quillin, M. L., Anstrom, D., Shu, X., O'Leary, S., Kallio, K., Lukyanov, K. A., Remington, S. J. The kindling fluorescent protein from Anemonia sulcata: Dark state structure at 1.38-Å resolution. Biochemistry, in press). Ehrlenmeyer lactonization and oxidation of the methylene group attached to the heteroaromatic moiety with selenium dioxide were used at the key stages of the synthesis. The spectral properties of the model chromophore in solution and their dependence on the pH and polarity of solvent were investigated. In water, the chromophore was found to exist in two forms, neutral and anionic, with pKa = 7.1. In dimethylformamide solution, the spectral properties of the anionic form closely match those of the native protein, demonstrating that under these conditions, the compound is an excellent model for the chromophore within native asFP595.

Summary of Personnel Commitments

During all term of Project # 2325p researcherss and technical personnel of Institute are involved in experiments and other task of the Project in accordance with the Work Plan and the Work schedule.

Specialists involved in the project:

Personnel Category	Number of specialists	Work – months	Remarks
Category 1	1	13,7	
Category 2	8	208,55	

Equipment Acquired during the term of Project 2325p

	Description of item	Qnt	Unit cost	CUR	Cost, USD
1	Monitor 17" Samsung 753DFX	1	230	USD	230
2	P4-1700(ATX)/256/512/60Gb/3.5/DVD-ROM 16/SB Audigy/128Mb/Spk	1	1 288.00	USD	1 288.00
3	Spectrophotometer Cary 50 Bio UV-VIS with Microcell 2/pk and Cary Win Bio Software	1	8 861.00	USD	8 861.00
4	Analitical balances OHAUS	1	20 192.70	RUB	639.39
5	Sheiker ELMI, S-3 micro	1	10 208.00	RUB	323.23
6	Eppendorf Centrifuge Minispin	1	28 391.00	RUB	898.99
7	Microcentrifuge vortex CV-1800	1	4 625.50	RUB	146.46
8	RoverBook Explorer E410L: P4-2400/512/256/30Gb/DVD-ROM-CD-RWSB/32Mb/FM-56.6/FEther-32/14.1" TFT/Spk/MS DOS	1	1 334.00	USD	1 334.00
9	Amplificator PTC-150 MiniCycler thermal cycler with Hot Bonnet heated Lid, holds 16x0,5 ml tubes, MJ Research, Inc. Cat.# 1151	1	3 295.00	USD	3 295.00
10	Rotor F-45-24-11, Cat.Eppendorf 5425 725.000	1	240	EUR	296.35
11	Centrifuge 5415R, Cat.Eppendorf 5426 000.018	1	2 930.00	EUR	3 617.96
12	Laser printer HP LaserJet 1200 with USB-cable	1	379.1	USD	379.1
			Total:		**21 309.48**

Director
of Shemyakin - Ovchinnikov Institute of
Bioorganic Chemistry, RAS

Vadim T. Ivanov

Manager of Project № 2325p

Sergey A.Lukyanov